MEASUREMENT OF LINEAR POSITION USING A MAGNETOSTRICTIVE WIRE

Thesis Submitted in Partial Fulfillment
of the Master of Science Degree
Faculty of Engineering
University of Cape Town

A.J. PENNINGTON, BSEE, UNIVERSITY OF WASHINGTON, 1964

1986

ACKNOWLEDGEMENTS

The author wishes to thank Professor J.F.W. Bell for proposing the thesis topic and for countless hours of instruction and aid as well as MINTEK and the University of Cape Town Department of Electrical Engineering for providing facilities and equipment.

Also the author would like to thank his wife and family for a year of understanding when he was immersed in the project.

SUMMARY

This thesis reports the details of construction and testing of a linear position measuring device and subsequent experimentation with the system.

The design goals established were to construct a measuring device using established TTL devices, proven interfaces, ultra-reliable noise-clean circuits, inexpensive components and to be based on transmission of magnetostrictively generated pulses in nickel wire. In addition it was to be able to operate in a harsh environment (e.g. underwater) where alternative devices would not function. While an accuracy objective was not established, it was hoped to be able to push accuracy near to the theoretical resolution.

A prototype measuring device was constructed consisting of a stretched nickel wire threaded through a transmitting coil and three receiving coils together with transmitting, receiving, timing and interface circuitry. The nickel wire was mounted on an optical bench with one receiving coil mounted to a moveable trolley. This configuration facilitated calibration and testing. The system was interfaced to a microcomputer via an IEEE 488 GPIB controller and calibration, testing and position measurement performed with appropriate computer programmes.

Testing, calibration and operation in a variety of physical configurations and under varying environmental conditions verified that the measuring device fulfilled all design requirements. With clock circuits operating at 10MHz, resolution was 0.5mm and without electronic error correction techniques, absolute accuracy was $\pm$ 2.5mm. The system was demonstrated to operate at the limit of LS chip technology of about 30MHz with a resolution of 0.17mm and the maximum frequency at which it would operate was 42MHz. At the same time calibration error was reduced to $\pm$ 1mm by applying the calibration error curve to correct the raw reading. This was possible since

calibration error, once measured, was very predictable. $\pm$ 1mm was considered the lower limit of total error and could only be achieved with relatively complex counting circuits, since pulse detection by threshold crossing introduced errors up to $\pm$ 2mm. These special counting circuits were demonstrated to reduce error as predicted.

It was concluded that linear position measurement using magnetostrictive wire is a viable alternative to many other methods for distances up to about 60 meters and is decidedly superior under adverse environmental conditions. Typical applications would include positioning cranes and similar machines that operate on tracks.

INDEX

CHAPTER 1

INTRODUCTION

1.1 Rationale for the Investigation

Most linear position measuring devices suffer from some basic limitation. Lasers are not effective under water or in obscured atmospheres. Lead screws become mechanical nightmares when used for extreme distances, require substantial support and are expensive to produce and prone to wear. Inductive pickups are generally fragile, and must be protected from industrial conditions such as swarf accumulation. Calibration for most devices requires submittal to a calibration laboratory or time consuming work in the field. A need was seen then for a robust, self calibrating, inexpensive, linear position measuring device that could operate under conditions not favourable to other devices.

1.2 Design Objectives

The preliminary objectives were:

1.2.1 The design was to be inexpensive. It should use only cheap, tried and true, components. The scale of integration was to be limited to simple chips such as one-shots, counters, oscillators, buffers and the like.

1.2.2 Control should be effected by a microprocessor. However, for the experimental version, a microcomputer would be used in order to enhance data taking and experimentation.

1.2.3 The system should be immune to electrical noise.

1.2.4 All logic should be TTL and generally LS devices were preferred.

1.2.5 The principal of operation was to be transmission and detection of magnetostrictively generated pulses on

nickel wire. It was felt that the pulse velocity (approx. 5000 m/s) and the ability to produce a fast rising leading edge would provide the required accuracy and measurement rate (10 per second) while use of a moderate diameter nickel wire would produce a robust device. One and one half and two millimeter diameter wires were available.

1.2.6 The device was to operate in harsh environments. The two harshest environments considered were underwater and oil soaked metallic swarf.

1.2.7 Negligible operator training would be necessary to obtain measurements. The device would be self calibrating and the set-up could be effected from a simple one page diagram and instructions. In essence, the device was to have immediate commercial applicability.

1.3 Design Considerations

References (1), (2), (3) and (4) were used as background material in order to establish preliminary design approaches. Based on the preliminary design objectives some preliminary design approaches were considered and these included:

1.3.1 Since electrical noise immunity was desired, a low impedance output preamplifier would be placed on the nickel wire at the receiving coils.

1.3.2 A basic requirement is that velocity be uniform along the length of the nickel wire. The velocity is dependent on, among other things, temperature, tension, magnetisation and wire characteristics such as annealing or cold working. The design should make the system self

calibrating and therefore errors will arise only from any non-uniform properties of the wire. That this is so can be demonstrated using Figure 1.3.a.

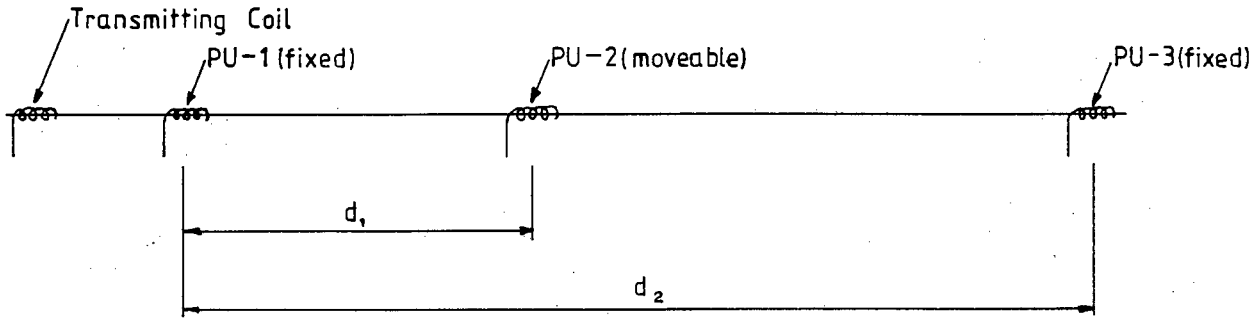

Figure 1.3.a

As a linear approximation, the velocity of the pulse can be considered to be

$$V = V_b + (V_b C_k \triangle C) + (V_b C_T \triangle T)$$

Where

V = Propagation velocity

V_b = Base velocity (4700 m/s for annealed Grade 200 at 40°C)

C_k = Velocity correction coefficient for temperature (1/°C)

$\triangle C$ = Temperature difference from 40°C

C_T = Velocity correction coeficient for tension (1/MPa)

$\triangle T$ = Tension difference from a base tension

and only small deviations of temperature and tension are considered. Referring to Figure 1.3.a, the time t_1 required for the pulse to travel the distance d_1 is d_1/V_1 and the time t_2 to travel the distance d_2 is d_2/V_2. Writing

$$V = V_b (1 + C_k \Delta C + C_T \Delta T)$$

gives

$$t_1 = d_1/V_b (1 + C_k \Delta C_1 + C_T \Delta T_1)$$

and

$$t_2 = d_2/V_b (1 + C_k \Delta C_2 + C_T \Delta T_2).$$

We can take the ratio t_1/t_2 and if the temperature is constant along the wire (which it should be), the effect of temperature and tension divide out (as will any factors which uniformly affect velocity along the wire). For this reason it was decided to structure the circuit to provide counts equivalent to the times t_1 and t_2 and to calibrate the system with an equation of the form

$$D = K_1 C_1/C_2 + K_2$$

where C_1 is the count equivalent to t_1 and C_2 is the count equivalent to t_2. Once calibrated, the system would then be "self-calibrating" with respect to any disturbances that produce velocity changes that are uniform along the wire. It is noted that calibrating in this manner should make the system relatively insensitive to the position of the first fixed receiving coil.

1.3.3 Velocity of sound in nickel wire does in fact depend on many other factors which may not be uniform along the length of the wire. Some of these include metal purity, cold worked or annealed conditions and magnetisation. As a design approach it was decided to use pure nickel

(grade 200 or 201 - ASM Metals Handbook), stretch to achieve very straight wire, if necessary anneal by heating either directly or indirectly and demagnetise with 2KHz either via the moveable receiving coil or indirectly with an auxiliary AC magnet. First, however, the device was to be built and the non-linear effects quantified to determine exactly what actions would be required. It was hoped that drawing the wire from the ingot would have produced uniform characteristics.

1.3.4 A convenient way of transmitting and detecting a mechanical pulse on magnetostrictive wire is via electrical solenoids. The magnetostrictive effect is non-linear and a magnetic field (bias) is required in order to operate the transmitting and receiving coils in a region that maximises the magnetostriction (strain) and therefore maximises the strength of the transmitted and received pulses. Also since a magnetostrictively generated pulse is a physical (sound) pulse travelling through the wire, a coil and magnetic field are required to generate an electrical pulse from the received mechanical pulse. Since demagnetising of the nickel wire might be desired it was decided to prepare two moveable pickups incorporating as bias permanent magnets and electromagnets. Then, if demagnetisation were required both a direct and indirect option would be available. For simplicity the direct option would be more desirous.

1.3.5 There are few (one or two) sources of pure nickel wire. Since four meters length of 2mm diameter wire were available it was decided to concentrate entirely on this wire. An optical test bench with three meter scale and a moveable trolley was available which prompted an immediate decision to build the device onto the optical

table. This left only about one meter of wire for initial experimentation and testing and as a result much of the preliminary work was done on 1.5mm diameter wire. There was no reason to expect that the results would not be directly applicable.

1.3.6 The desired signal output from the detection coils is a square wave. To approximate a square wave a large signal with very fast rise time was to be achieved. This signal would be converted to TTL at a fixed threshold and therefore short rise time would be required in order to minimise error. Additionally, minimum change (due to loss) in pulse profile over the entire length of wire would minimise error since the threshold crossing would remain essentially constant. Since an electrical square wave output was desired a mechanical square wave should be transmitted along the nickel wire. Practically this means that maximum change in strain with respect to time should be achieved.

1.3.7 Some options to be investigated are shown in Figure 1.3.b, 1.3.c and 1.3.d. Since it is possible to transmit and receive on the same solenoid coil, the configuration of Figure 1.3.b could be used. The base time t_2 would then be the round trip time and the time t_1 would be the travel time from transmitter to moveable pickup. In Figure 1.3.c the moveable pickup transmits and receives echo pulses from either end. This is potentially the simplest arrangement since only one coil is required. However, since the signal with time t_1 could arrive after the one with time t_2, a method to resolve the ambiguity would have to be devised. Figure 1.3.d shows a three coil arrangement which minimises problems with ambiguity.

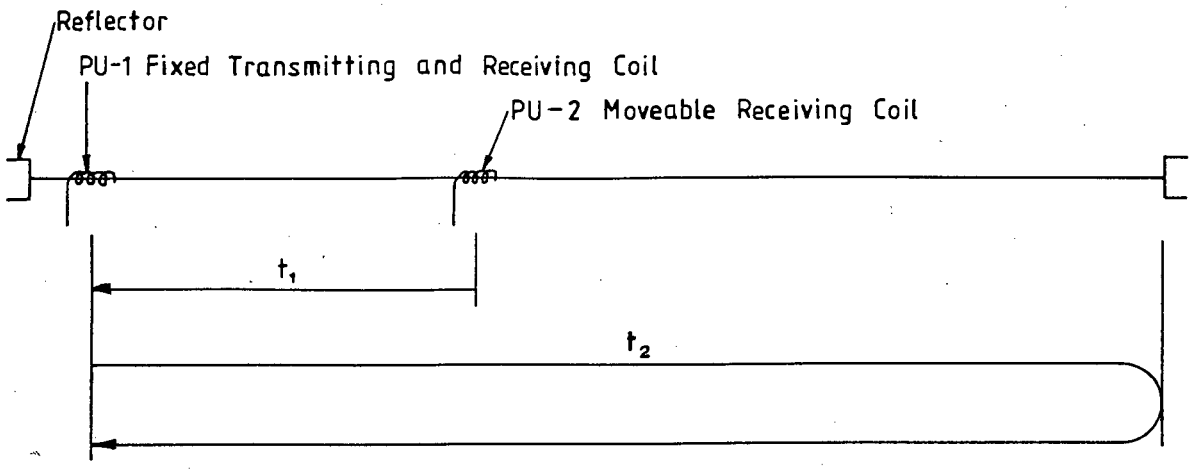

Figure 1.3.b

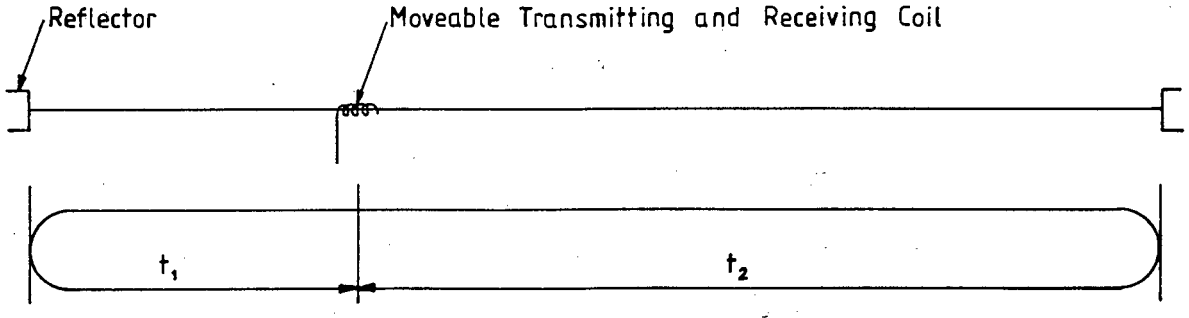

Figure 1.3.c

Note that $(t_1 + t_2)$ is constant and provides the fixed baseline and also a double amplitude signal.

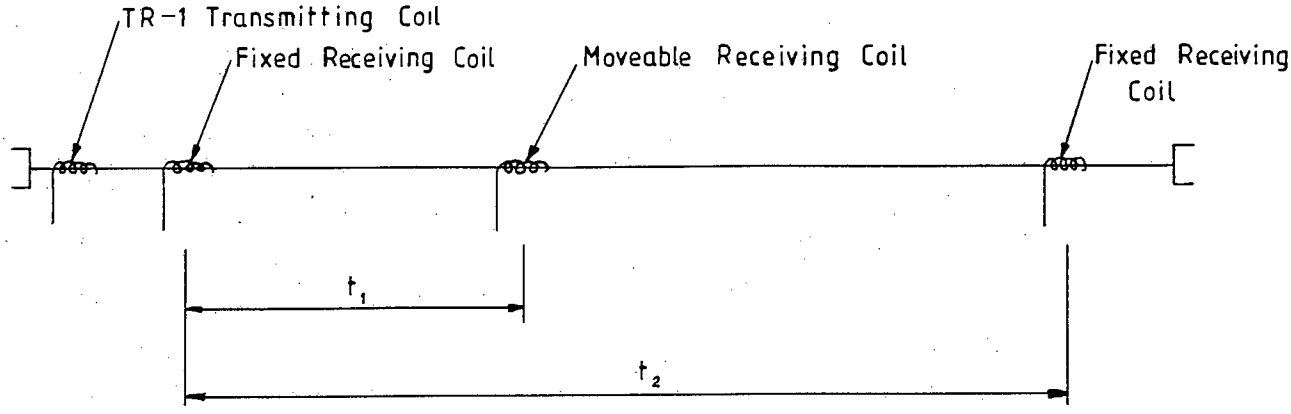

Figure 1.3.d

It was decided to start with the geometry of Figure 1.3.d since it provides the greatest flexibility for investigating system changes.

CHAPTER 2

PRELIMINARY EXPERIMENTATION

2.1 Transmitting Effectiveness

2.1.1 It is desired to magnetostrictively induce a mechanical pulse into the nickel wire in such a manner that it approximates as closely as possible a square wave. A typical receiving coil and exaggerated pulse are shown in Figure 2.1.a.

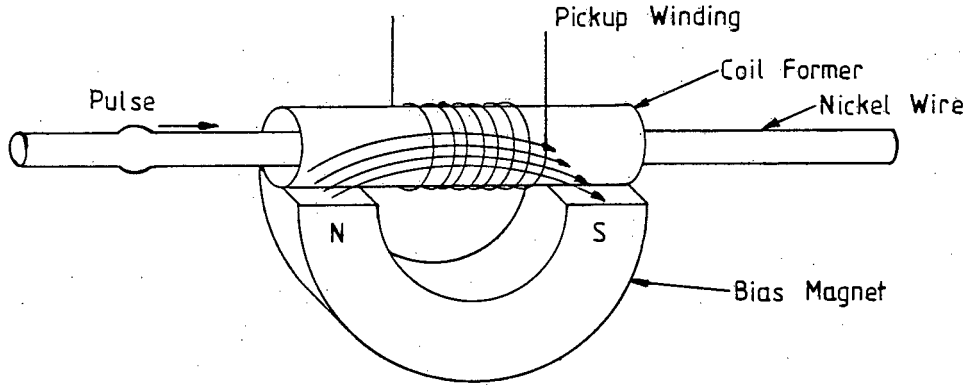

Figure 2.1.a

In order to induce maximum voltage in the receiving coil, the mechanical pulse leading edge should be as sharp as possible. Since flux (Φ) is proportional to strain(s) and voltage is proportional to $Nd\Phi/dt$, voltage is proportional to NdS/dt. Velocity on the wire (for a given pulse) is constant, and therefore the maximum strain (dl/l) produces maximum $d\Phi/dt$ in the receiving coil. For the transmitting coil then, proper bias will produce maximum (dl/l) for a given ΔB and a square wave of current will produce the maximum ds/dt. This suggests a low

impedance circuit matched to a current source. Theoretical response of various coils was investigated using methods of Refences 5 and 6. The transmitter system was designed empirically by driving various combinations of coils with various current sources and observing the received wave form. The current sources themselves were gated on and off with TTL and discrete transistor timing circuits. The starting point for empirical determination was a transmitting system described in reference (1). The driving circuit for experimentation was built using a 74LS629 VCO followed by a 74LS221 MONO input to a 2N2222A NPN transistor which switched a TIP32C in series with the coil and $\pm$ 15VDC rails. This allowed testing each coil with variable pulse width signals. Fifty coils were prepared of various lengths, numbers of turns, gauge of wire, numbers of layers and all on coil formers made from the ink tube of BIC ballpoint pens. These ink tubes were found to closely fit the 2mm diameter wire and were available. A thinner walled, harder tube would have been preferable but none could be found. A receiving coil was obtained from a past project and fixed in position. The pickup output was input to one trace of a dual beam scope and the settings and geometry kept constant. Then each coil was tested at a fixed location on the wire with respect to the pickup coil. Each test consisted of varying the pulse width and observing the received signal. First the test was done with no transmit coil bias and then repeated with various permanent magnets used to bias the wire. This empirical process was chosen over calculational methods for several reasons. Firstly, the thesis project goals did not include designing an effective transmitter under all conditions but rather selecting a transmitter that would demonstrate the method of linear position measurement. Secondly, calculational

design of the smallest, biased, solenoid that produces maximum ds/dt (s=strain), and for a given velocity of propagation, the maximum $d\Phi/dt$ in the receiving coil is extremely complex. The empirical method on the other hand is very simple, and for the purpose, quite speedy. One effect that was noted and guarded against while experimenting with the unterminated wire was the pulse addition due to placing the coil center at 1/4 wave length from the unterminated or open end of the nickel wire. It is possible to obtain a 2π phase shift (π for open end reflection and π for the $2\pi/4$ positioning) and reinforce the transmitted pulse. Since the final wire assembly was to be fixed at both ends, this effect was not desired. A small resistor in series with the TIP32C and coil was used to measure voltage wave forms and infer coil current and energy. The test set up is shown in Figure 2.1.b.

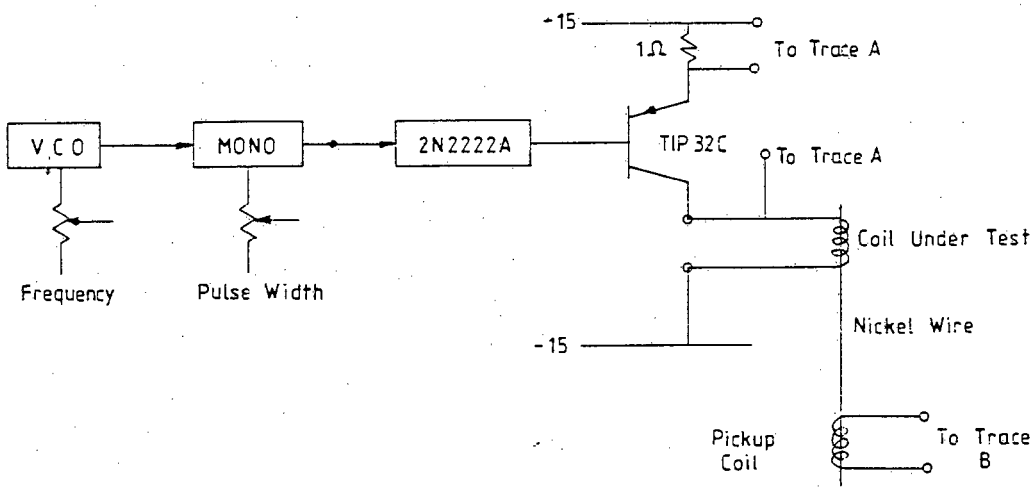

Figure 2.1.b

2.1.2 The test setup was also convenient for measuring transmission velocities and detecting velocity anomalies in the nickel wire. For measuring velocity the distance between coils was measured and the time difference read from the scope. For detecting anomalies, the coils were fixed and the received pulse placed over the transmitted pulse on the scope. Then the wire was slowly moved through the coils. Any velocity difference was noted as a pulse displacement. In this manner the average velocity over the distance separating the coils could be measured. The velocity of sound in the wire is approximately $5mm/_{microsecond}$. Even with small lengths of wire, deviations in velocity with length are easily detected. Pieces of wire were heated, magnetised and cold worked (by bending) and the effects on velocity noted.

2.1.3 The setup was somewhat sensitive to damping if the coil formers or other objects firmly touched the nickel wire. In order to produce consistent results the wire was placed on three foam pads and care was taken to ensure that the coil formers were free on the nickel wire.

2.1.4 The final transmitting coil arrangement is shown in Figure 2.1.c and the summarised results of this effort are shown in Figure 2.1.f. The circuit used for experimentation was selected as the final circuit based on the fact that it provided satisfactory performance. By changing the bias and coupling of the 2N2222A, the coil voltage could be made either 15 volts or 30 volts.

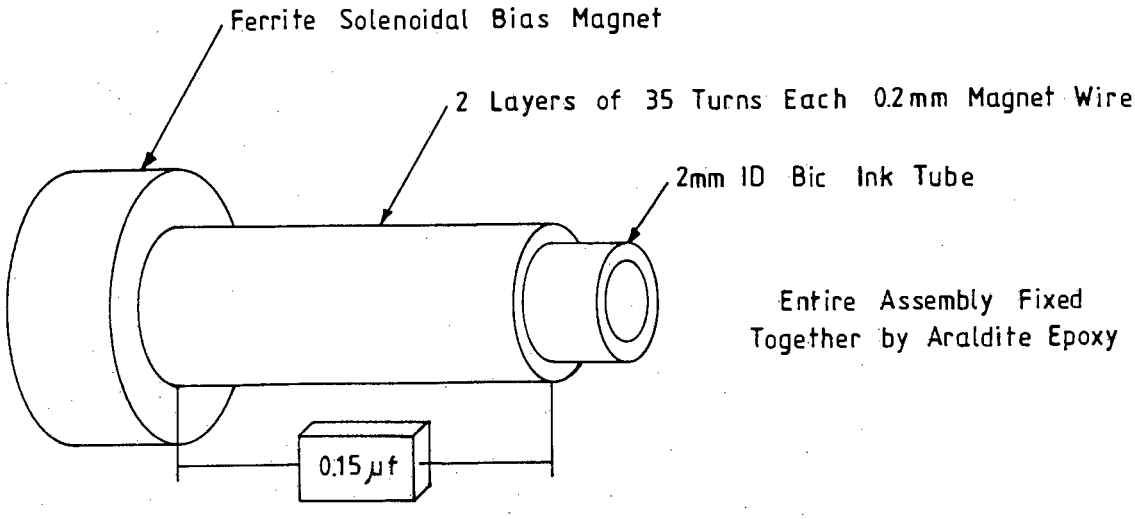

Figure 2.1.c

2.1.5 The final series of tests was performed with the coil arrangement shown in Figure 2.1.d. This arrangement was used in order to precisely define the transmitted pulse. Other arrangements resulted in a noisier transmitted pulse, with more ringing than was desired.

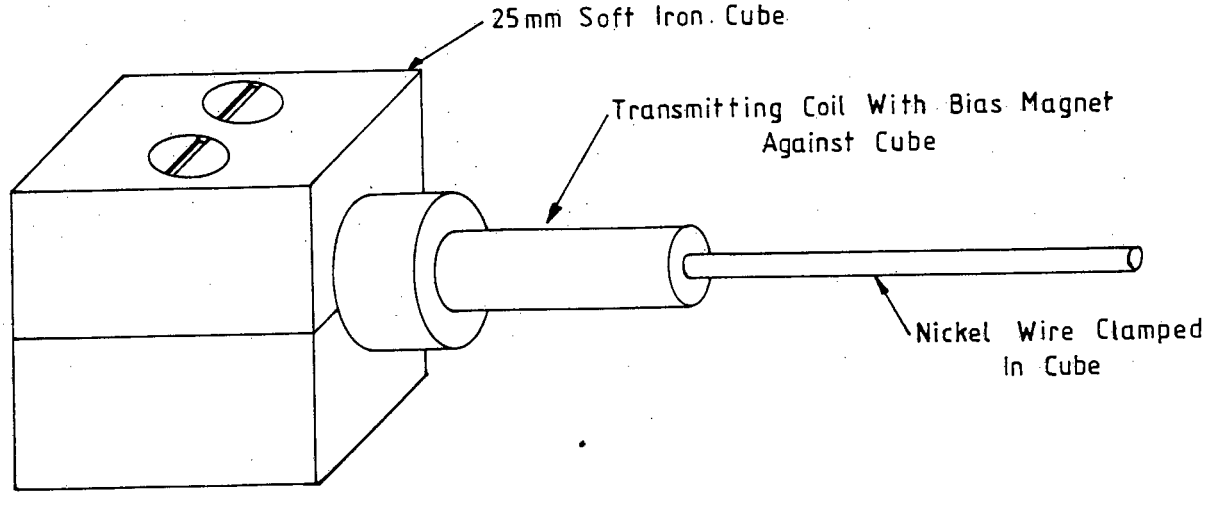

Figure 2.1.d

2.1.6 Figure 2.1.e shows the receiving coil output shape after amplification when transmitting into the best transmitting coil. Detection will be made on the fast rising positive leading edge. Several transmitting coils were constructed to demonstrate that this pulse shape could be consistantly obtained each time with the coil shown in Figure 2.1.c and the arrangement of Figure 2.1.d.

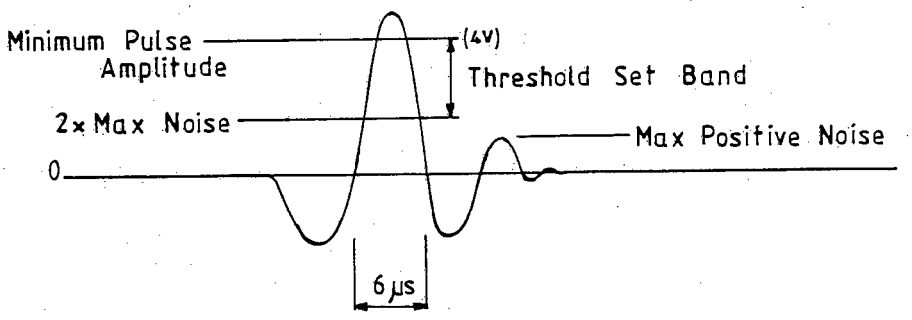

Figure 2.1.e

2.1.7 Figure 2.1.f shows an example of final results for coils which gave the desired pulse shape out of the pickup coil. The points plotted are maximum values for all types of bias magnet arrangements including no bias and for all values of parallel capacitance. Peak values were obtained with a close fitting ferrite magnet on the end next to the reflecting cube. This magnet was polarized with flux coming from the face. The best rise times and cleanest pulses were obtained with 0.15 microfarad parallel capacitance. The transmitting coil was designed by:

- preparing many coils with different lengths, wire sizes and number of turns
- measuring performance with identical test geometry each time
- Biasing each coil with the same magnets in all logical ways
- plotting the results and selecting the optimum coil and configuration.

Figure 2.1.f illustrates data for a coil former of 3mm diameter and 12mm length using a 2mm diameter nickel wire and pulse duration of 8 microseconds.

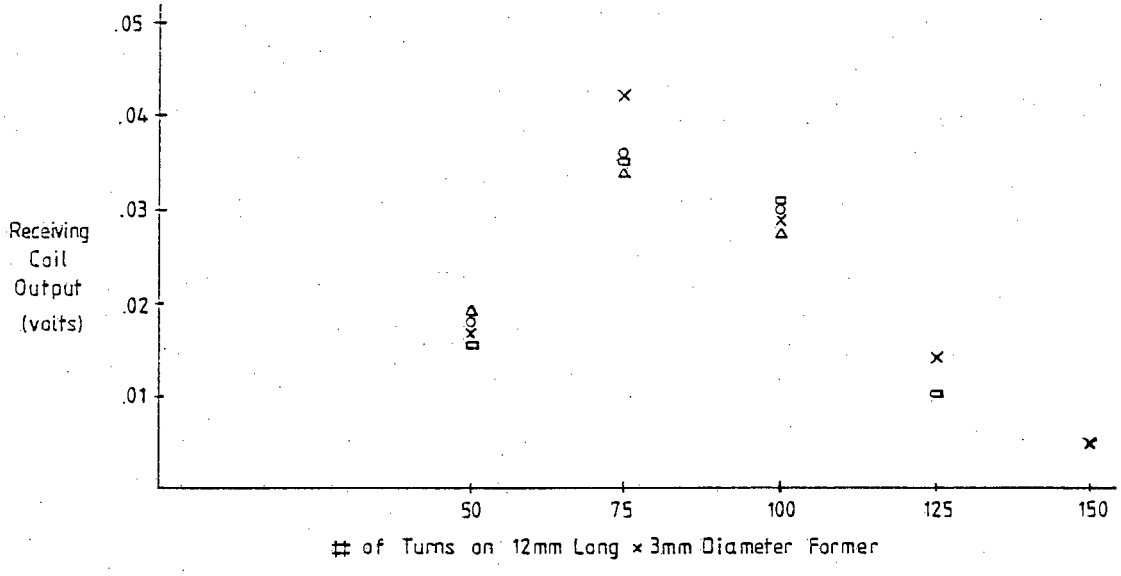

Δ = .04mm Enameled Magnet Wire
× = .2mm Enameled Magnet Wire
o = .08mm Plastic Coated (solderable) Magnet Wire
□ = #28 Enameled Magnet Wire

Figure 2.1.f

COIL PERFORMANCE FOR VARIOUS WIRES

2.2 Receiving Effectiveness

2.2.1 Detecting the pulse is somewhat different from transmitting the pulse in that the transmitting electromagnet will generate a mechanical pulse but the pulse will not generate a magnetic field. It is therefore a necessity to use bias magnets with the receiving coil. At the same time the optimum bias point should be used. The distortion (pulse) of the nickel wire passing through the bias magnet's field causes a change in flux $d\phi/dt$ which results in an induced voltage $Nd\phi/dt$. The change in flux linkage is related to how the pickup coil is wound and placed with respect to the magnetic field and the nickel wire as well as the strength of the magnet. A check of relevant literature showed that the best geometry involved winding a solenoid of many turns of fine wire around the nickel wire. However, many types of bias magnet arrangements had been tried but no optimum placement was indicated. Figure 2.2.a shows some considerations used in biasing the receiving coil.

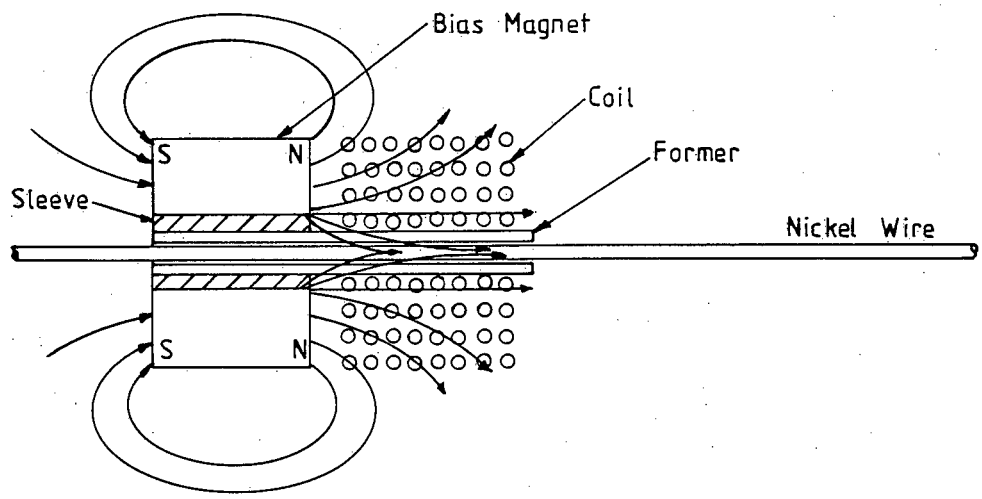

Figure 2.2.a

The same general considerations apply as applied to the transmitting case. Now, however, a large voltage output is desired. That means many turns of fine wire resulting in a high impedance coil may be used. Ideally, maximum change in ϕ should result when the pulse passes by the receiving coil. Since the nickel wire is ferromagnetic, the flux will concentrate in the wire. Any change in shape of the wire will change the flux. This indicates that a short multi-turn coil placed close to the bias magnet should be most effective.

2.2.2 A large assortment of permanent magnets was available but the field strength was not known for any of them. Also, no convenient apparatus was available to measure field strength. As a result, the effects of all available magnets in every conceivable orientation were checked. At the same time cognizance was taken of the physical restrictions imposed by the requirement to install and use the device. These requirements included ability to position all of the coils and ability to freely move the coil PU-2. The three arrangements which proved satisfactory are shown in Figures 2.2.b, 2.2.c and 2.2.d. In each case the nickel wire is physically prevented from sticking to the magnet. The arrangement shown in Figure 2.2.c provided a larger signal output than the others when it was not against the reflecting cube. When against the cube its performance was only marginally better. All coils produced slightly larger signals when their bias magnet field direction was opposite to that of the transmitting coil bias. The final selection was to use the arrangement shown in Figure 2.2.b for the fixed receiving coils and to use the arrangement of Figure 2.2.d for the moveable receiving coil. The moveable coil had to be hard mounted to prevent introducing error and the magnet geometry was ideal for mounting.

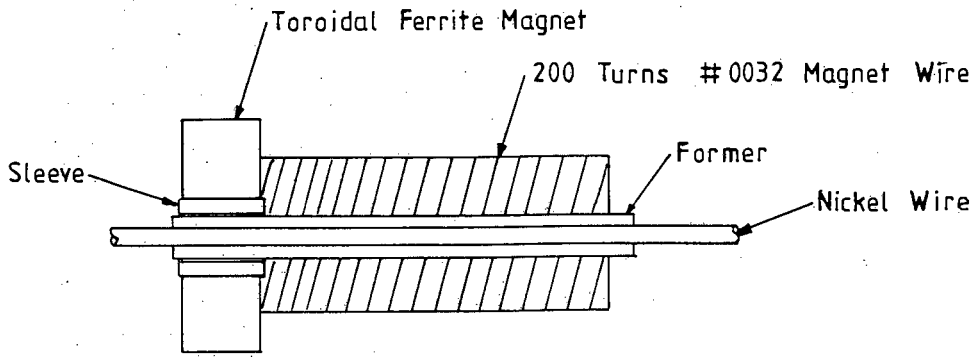

Figure 2.2.b

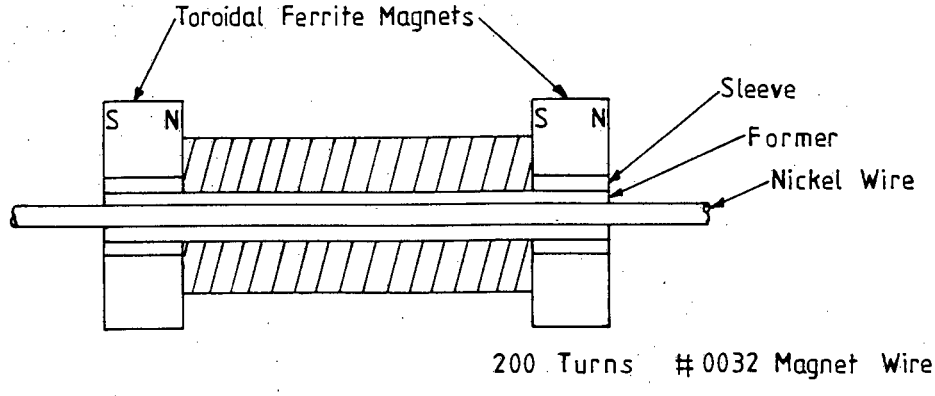

Figure 2.2.c

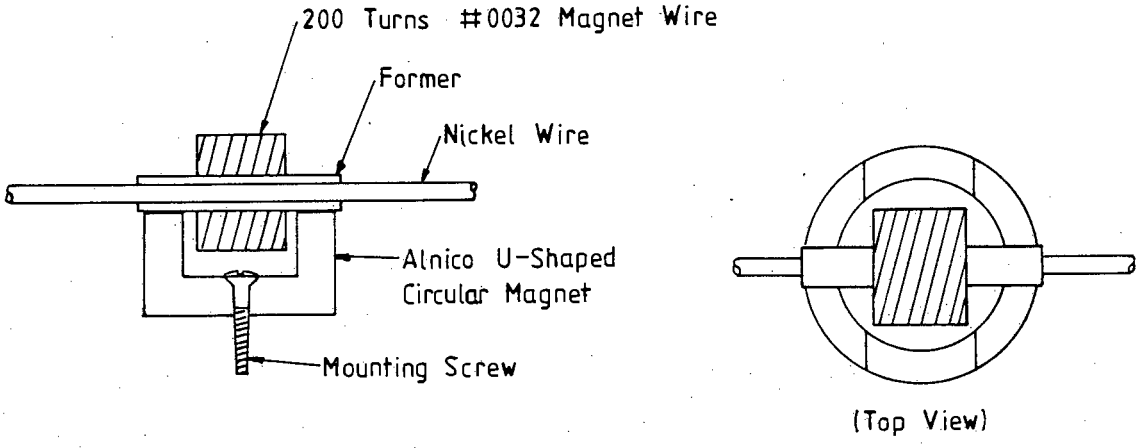

Figure 2.2.d

2.2.3 Immediately it was found that the nickel wire must either be demagnetised or else magnetised in the same direction as the bias magnets. Magnetising in the opposite direction reduced the output by more than a factor of five. Figure 2.2.e and 2.2.f show the results of locally magnetising the wire around the moveable receiving coil.

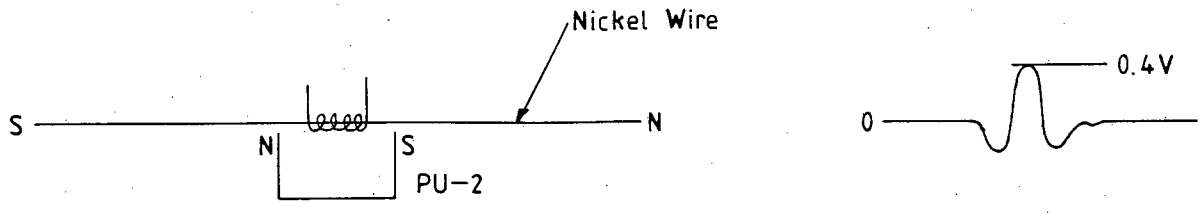

Figure 2.2.e

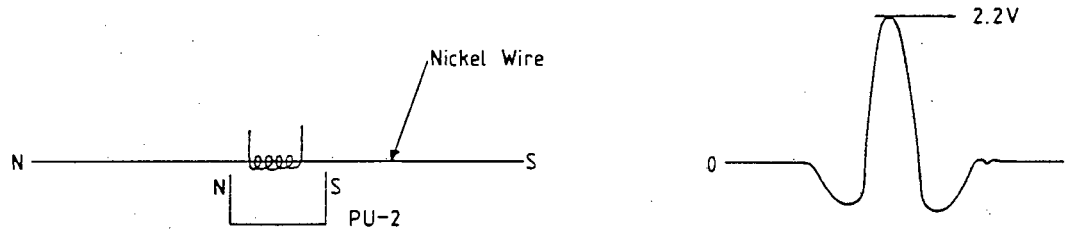

Figure 2.2.f

In both cases the wire was magnetised from optical trolley positions 160cm to 180cm by twenty strokes of a bar magnet of essentially the same strength as the alnico magnet used on the coil and the measurements taken at trolley position 170cm. The reading with the wire demagnetised was 1.2v peak. Additional discussion of locally magnetising the wire is found in Chapter 8.

2.2.4 Measurements made on the three meter long 2mm diameter wire showed that after ten reflections, the signal was still strong enough to detect unambiguously. This corresponds to greater than sixty meters which is about the distance over which a wire could be strung and a small enough catenary obtained to get the desired accuracy.

2.3 Final Approach

2.3.1 The test transmitting circuit discussed in Paragraph 2.1 and shown in Figure 2.1.b was selected as the final circuit. Oscillator frequency was made variable from 2Hz to 50Hz and output pulse width was made variable from

1 usec to 50 usec. These parameters were selected in order to allow transmission over thirty meters of wire and allow 250msec to process signals in a free running mode. It was not known at the beginning what the signal processing cycle time would be. Several IEEE 488 GPIB controllers were available and depending on how the signals were input, cycle times up to 225msec could be expected.

2.3.2 The transmit coil, receiving coils and reflecting cubes as shown in Figures 1.3.d, 2.1.c, 2.1.d, 2.2.b and 2.2.d were selected as the basic hardware around which the electronics would be built. The wire tensioning arrangement shown in 2.3.a was selected in order to be able to easily change components if one failed or if a different coil was to be tested later in the project. In order to change components, the soldered joint is desoldered and components are slipped on or off the wire. In a production model a suitable clamp would be used. With the optional insulator it is possible to pass current through the wire to stimulate a pulse in the torsional mode if desired. However, it had been decided early on that the torsional mode would not be suitable for this application, and in fact was not tested.

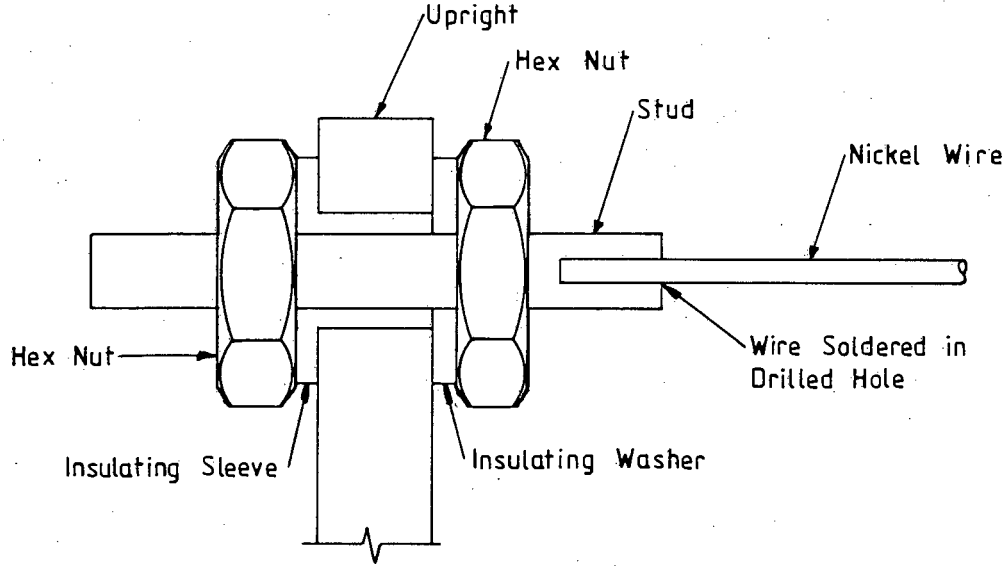

Figure 2.3.a

2.3.3 Most LS type TTL devices were found to operate reasonably well up to frequencies of about 30MHz. Above 30 MHz special circuits or much more expensive chips are required. Based on this information it was decided to build the circuits around 10MHz, but to test up to 30MHz. The simple approach shown in Figure 2.3.b was selected. The transmitter pulses the transmit coil and at the same time resets all the counter circuits. When the TTL pulse equivalent to the PU-1 pulse is received, two counters are started. The TTL pulse equivalent to the pulse from PU-2 stops the first counter and the one from PU-3 stops the second counter and signals the interface that the counting process is finished. At this point Counter-1 holds a count equivalent to the time for the pulse to travel from PU-1 to PU-2 and Counter-2 holds a count equivalent to the time to travel from PU-1 to PU-3. These counts when read by the computer via the interface allow computation of position of PU-2 using the formula $D = K_1 C_1/C_2 + K_2$ where the system calibration provides K_1 and K_2, and C_1 and C_2 are count-1 and count-2 respectively. Note that in this scheme no absolute distances need be known since any fixed scale applied to PU-2 will calibrate in units of the scale.

2.3.4 It was considered satisfactory to design a non-standard (IEEE-488) interface since only response to Service Request (SRQ), transmission of cycle start via Interface Clear (IFC) or Remote Enable (REN) as an option and sequentially reading data from the data bus were desired. Additional simplification was to be obtained by using ASCII characters to transmit numbers. Bus description and additional details are presented in Chapter 6.

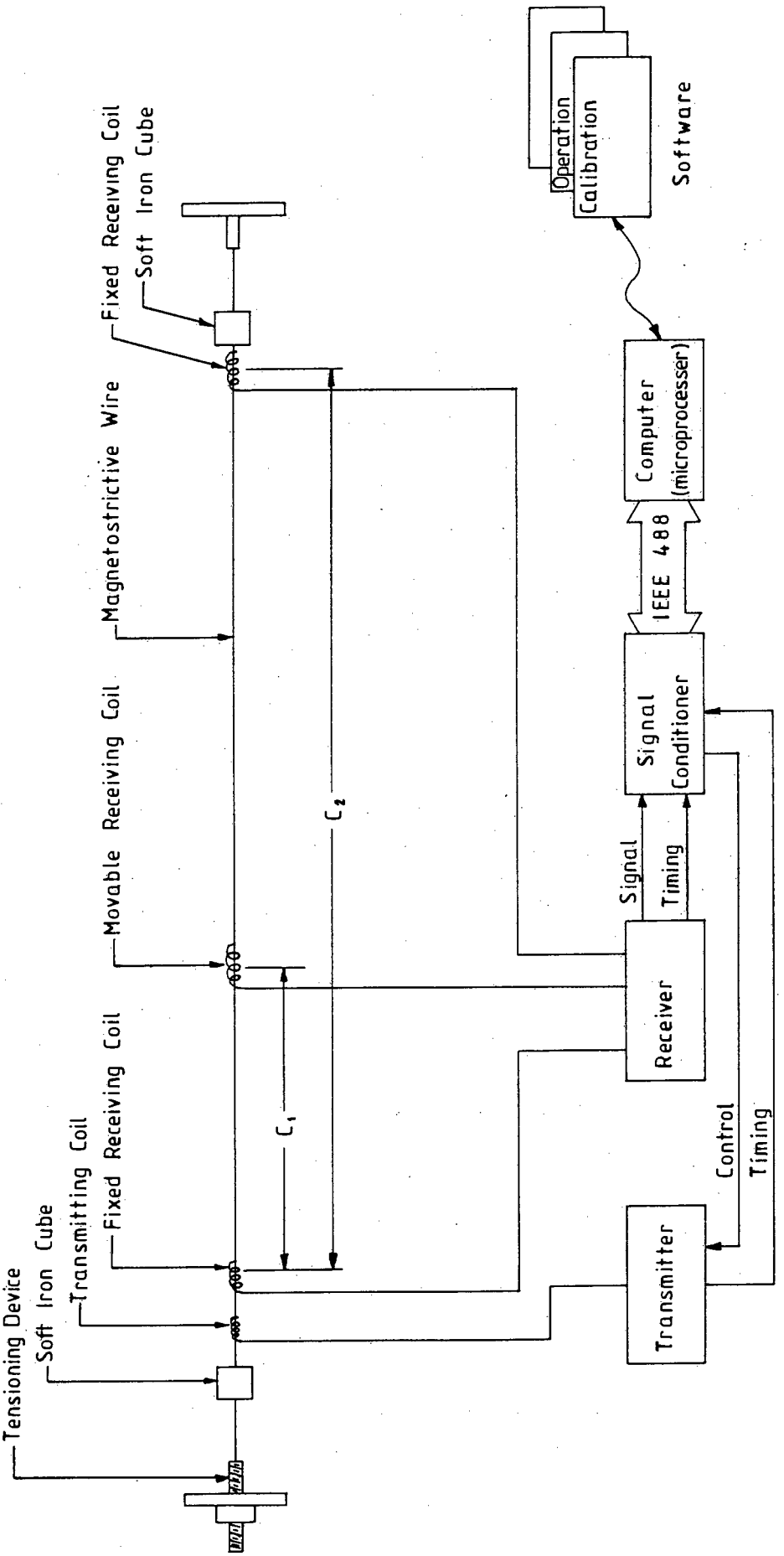
Tensioning Device
Soft Iron Cube
Transmitting Coil
Fixed Receiving Coil
Movable Receiving Coil
Magnetostrictive Wire
Fixed Receiving Coil
Soft Iron Cube
C_1
C_2
Transmitter
Receiver
Signal
Timing
Control
Timing
Signal Conditioner
IEEE 488
Computer (microprocesser)
Operation
Calibration
Software

Figure 2.3.b

CHAPTER 3

TRANSMITTING CIRCUITRY

3.1 Pulse Generation

Most of the transmitting circuitry was actually constructed during the experimentation phase discussed in Chapter 2. This chapter presents some additional considerations noted when the complete circuit was built and tested.

3.1.1 The functions of the pulse generating circuitry were to provide a free running pulse of 2 to 50Hz with pulse width of 1 to 50 microseconds and to provide a TTL reset pulse to the counting and interface circuits. An initial attempt was made to use chip circuits for all but the final output transistor. However, a common chip could not be found that would sink enough transistor base current to properly drive the TIP32C. As a result, the final two stages were built as discrete transistor stages. Several artificial constraints were allowed in the design. Common power supplies were $\pm$15VDC and +5VDC so the voltage supplies were fixed at these values. Vero board was selected for pilot circuits since it offered very easy construction. However, extra precautions had to be taken to keep transmitting noise out of the power supply and receiving circuits. Both the $\pm$15VDC and +5VDC were referenced to a common earth. Rather than optimise design by considering the transmitting coil and transmitting circuit as a unit, the two were developed independently. The transmitting circuit was developed first and it was assumed that a transmitting coil could be developed to match the transmitting circuit and give adequate system performance. As shown later, this approach was satisfactory.

3.1.2 In Appendix (1), the transmitting circuit schematic is shown. R_3 was brought out to the front panel to allow adjustment of pulse repetition rate and R_4 was brought out to allow adjustment of pulse width. C_4 and C_5 are large capacitors which serve as sources to drive the coil during the time that TR_2 is conducting.

3.1.3 Note that with the driving circuit shown in Appendix (1), the full 30VDC swing is not achieved. Originally the 2N2222A was arranged to cause the TIP32C to operate between -15V and +15V. However, it resulted in overdriving the first receiving coil by direct coupling and was modified to operate with a 15V swing. This resulted in a significantly higher dynamic resistance as shown in Section 3.2.1, but with overall satisfactory results. The output voltage to the coil when the coil was replaced with a ten ohm resistor is shown in Figure 3.1.a. This measurement was performed in order to estimate the TIP32C dynamic resistance.

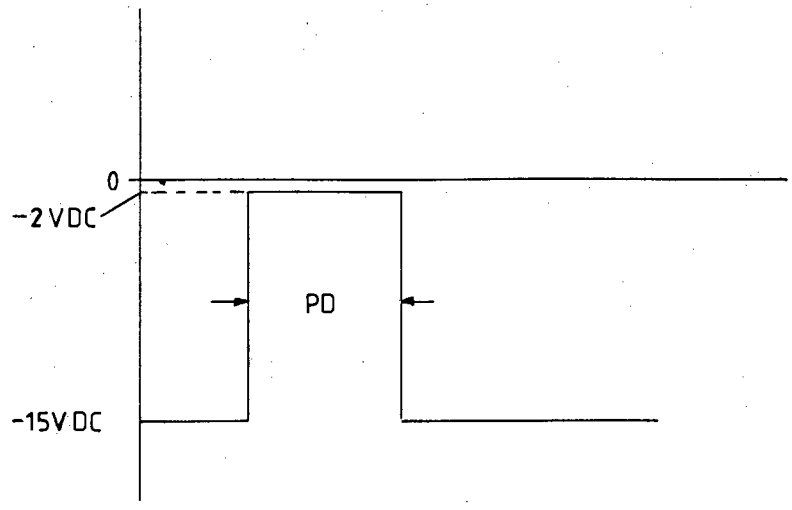

Figure 3.1.a

3.2 Transmitter Output Stage and Solenoid

3.2.1 The solenoid coil circuitry is shown in Figure 3.2.a

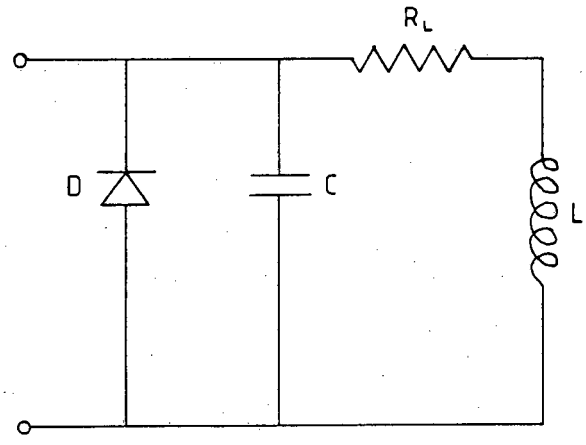

Figure 3.2.A

where the resistance of the coil is R_L (2.5 ohms for the final selection), the inductance measured at 1KHz and 10KHz is L (220 microHenries for the final selection) and the parallel capacitance used to match to the transmitter is C (0.15 microfarad for the final selection). A diode was used to prevent ringing but it was found to be unnecessary because of the low Q of the circuit and large t_{rr} of the TIP32C. A comparison of the output wave forms with and without the diode is shown in Figure 3.2.b. A switching glitch can be seen in the wave form but overall the transistor conducts until the voltage has returned to essentially -15VDC. The driving pulse duration was 10 microseconds for the wave forms of Figure 3.2.b.

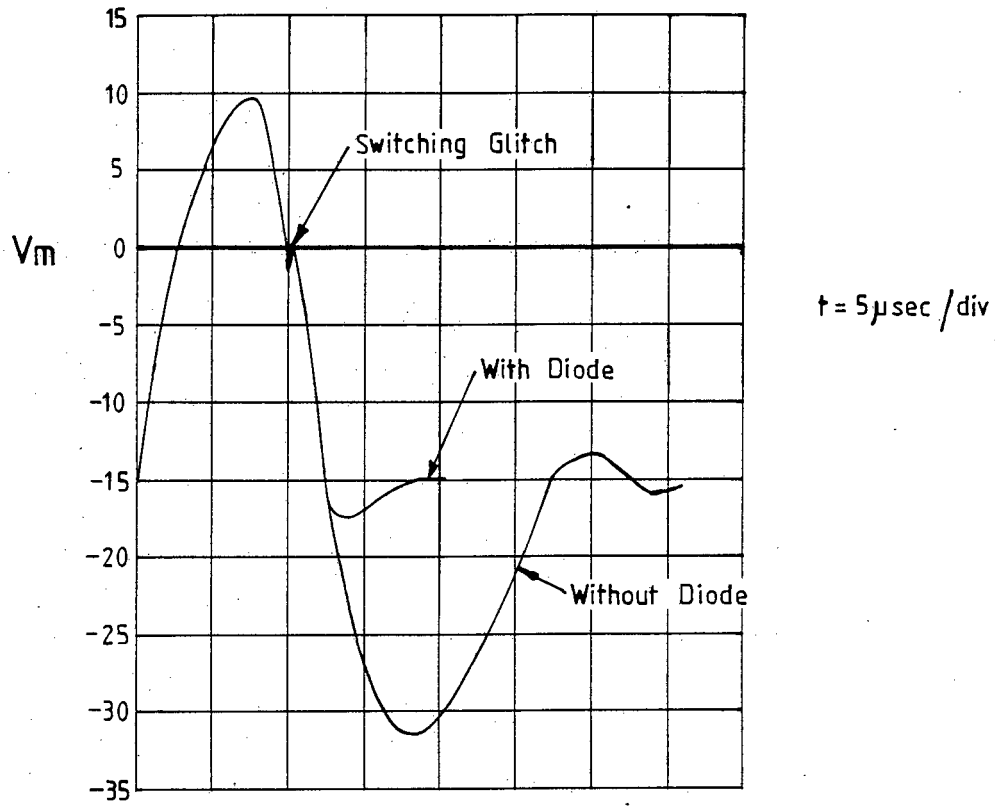

Figure 3.2.b

Using a first approximation of the TIP32C for large signals, the equivalent circuit of Figure 3.2.c is obtained.

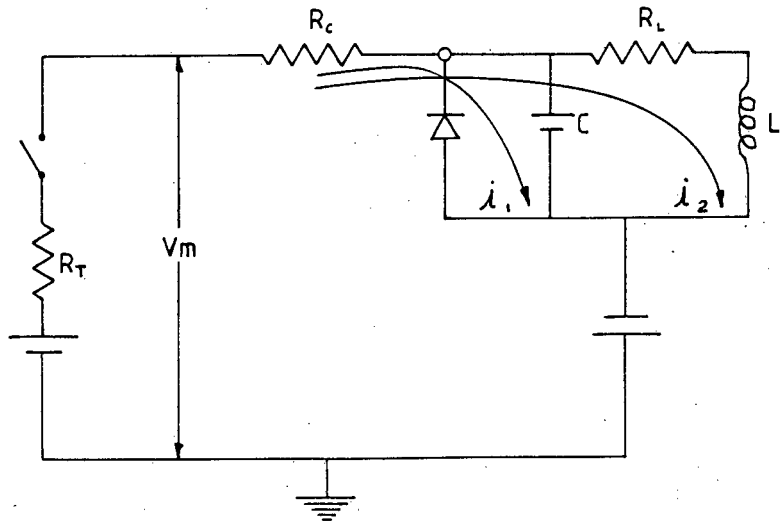

Figure 3.2.c

R_T = Dynamic resistance of the TIP32C = 12 ohms
R_C = Resistance of connecting leads = 0.8 ohms
R_L = Resistance of the coil = 2.5 ohms
C = 0.15 microfarad
L = 220 microHenries

R_T was measured by transmitting into a 10 ohm resistor and measuring the voltage drops. L was measured using the test circuit of Figure 3.2.d.

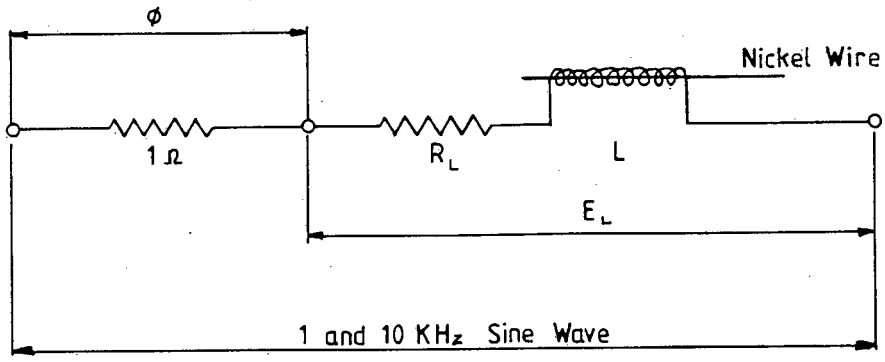

Figure 3.2.d

The response was checked for both 1KHz and 10KHz. The output of the 1 ohm resistor and E_L were displayed on the scope. Phase angle (ϕ) was read directly in microseconds and the current was numerically equal to the voltage across the one ohm resistor. In addition, for 1KHz, the current was measured directly with a Fluke 77 multimeter. The wave forms of Figure 3.2.e were obtained.

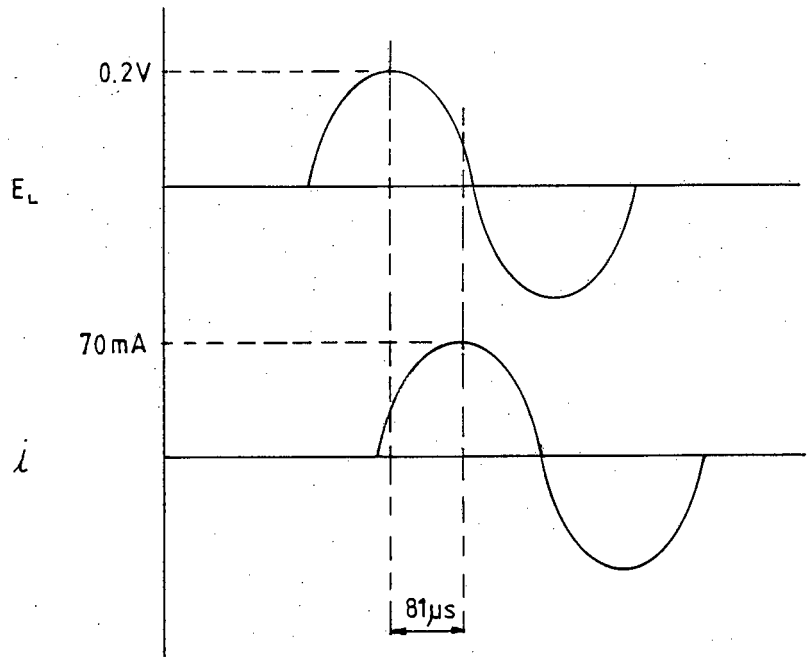

Figure 3.2.e (1KHz)

3.2.2 The circuit equation is then

$$\begin{bmatrix} 12.8+\frac{6.667\times 10^{6}}{S} & 12.8 \\ 12.8 & 15.3+2.2\times 10^{-4}S \end{bmatrix} \begin{bmatrix} I_1 \\ I_2 \end{bmatrix} = \begin{bmatrix} \frac{30}{S} \\ \frac{30}{S} \end{bmatrix}$$

for the period of time that the TIP32C is conducting. After TIP32C turnoff, the model becomes more complex and must include the reverse recovery time t_{rr}. This could be modeled by replacing the dynamic resistance and switch with a time varying resistance of $R_T = 12e^{(2.7\times 10^6)t}$. However, since the required results could be easily obtained empirically, there was no need of this complex model. A comparison of the waveform obtained to the waveform predicted is shown in Figure 3.2.f where

$$V_m = 6.47 - 42.28e^{-(423\times 10^3)t} + 37.68e^{-(85.5\times 10^3)t} \quad -15$$

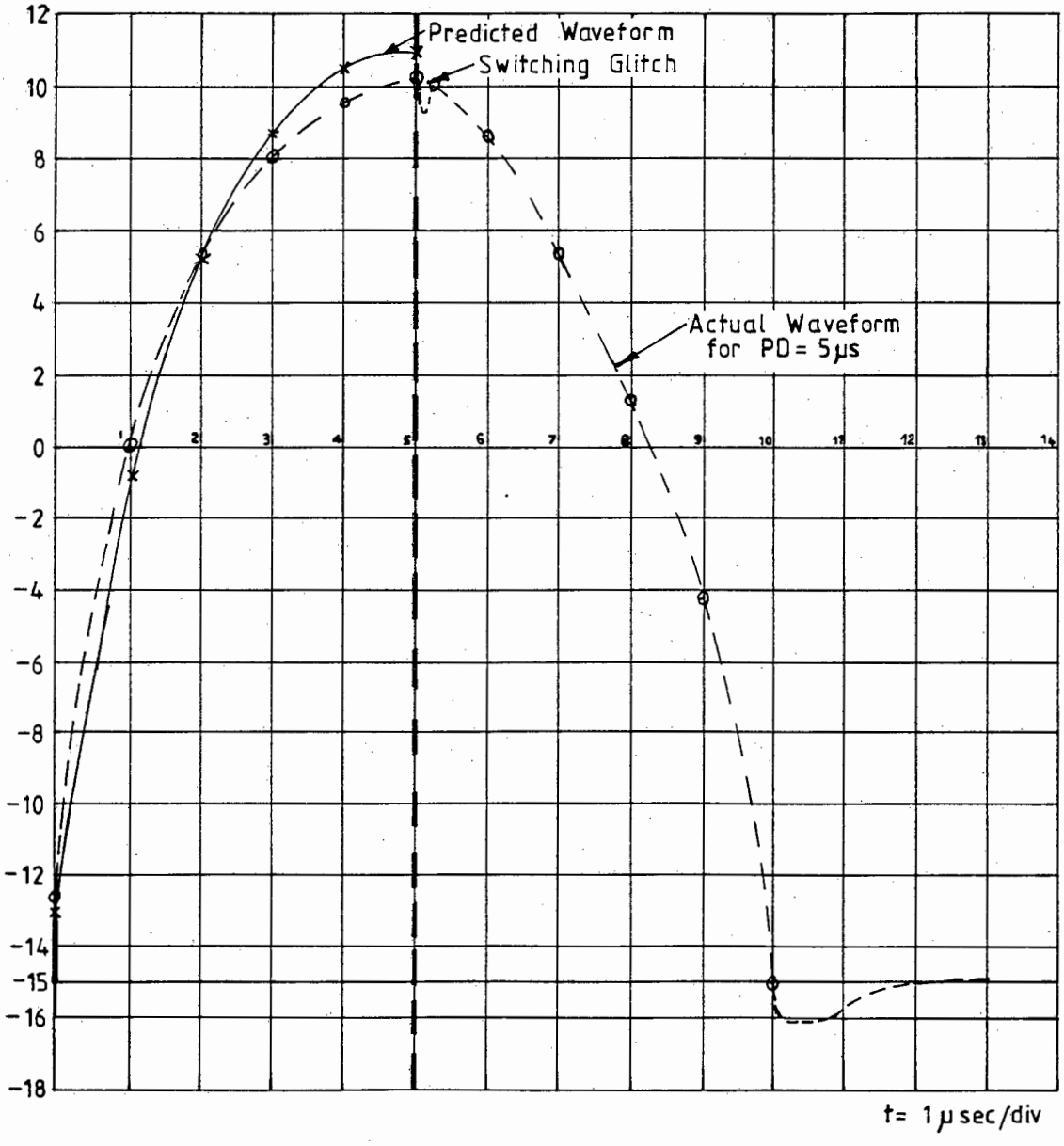

Figure 3.2.f

As discussed in Section 2, the optimum transmitting coil was selected by noting its effect on a receiving coil. This fact alone would make mathematical modeling for this application prohibitively time consuming. It was concluded then that the transmitting design objectives were met in a satisfactory fashion. The following facts are noteworthy:

- the coil former must be as thin and as tight fitting as possible. Otherwise, coupling to the wire is poor and the circuit tends to ring

- the number of layers of wire, length of coil and number of turns must be optimized, and must be matched to pulse length. Additional layers of wire once they get very far removed from the nickel wire have little effect. A longer coil has a higher inductive reactance, requires a longer pulse length and increases rise time. This adds error to the system

- the coil circuitry should be able to produce a large positive (or negative) going signal at the first crossing in order to optimise use of threshold detection. This would appear to rule out symetrical wave forms which cause the receiving circuit to oscillate several cycles before the peak voltage is received. Setting a threshold for the moving receiving coil would then be difficult. However, it was noted that the same effect of large unsymmetrical swing could be achieved by operating the amplifier with one half cycle in cutoff.

CHAPTER 4

RECEIVING CIRCUITRY

4.1 Pickup Coil and Preamplifiers

The receiving coils and circuits were actually developed during experimentation as discussed in Chapter 2. This Chapter contains additional information on the receiving amplifiers and then discusses the TTL conversion.

4.1.1 The functions of the pickup coils and preamplifiers were to detect the magnetostrictive pulse and supply a low impedance noise immune signal to the pulse shaping and counting circuits. Several geometries of coil were tested. In general the only parameters which greatly affected performance were the coil bias and coil length. All three geometries discussed in Section 2 and shown in Figures 2.2.b, 2.2.c and 2.2.d performed satisfactorily. They all produced the output wave form shown in Figure 4.1.a.

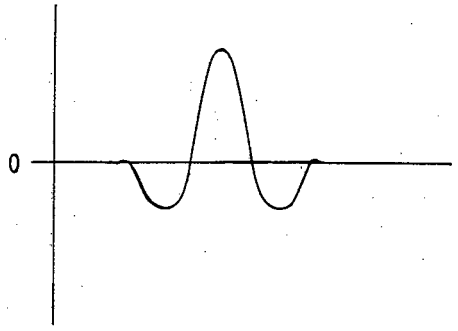

Figure 4.1.a

The first positive going crossing is followed by a large positive pulse which ensures that threshold detection will be successful. The final arrangement of bias magnets was based primarily on the ability to repeatedly construct receiving coils with identical characteristics. Bias was also supplied by electromagnets. However, it was found that they were too large and occasional noise in the electromagnet power supply was coupled into the receiving coil and caused false readings. In addition, in order to stop the noise, extra power leads were needed for the moveable receiving coil. This was not desirable.

4.2.1 In order to achieve low noise, low impedance output, it was desired to place at least one stage of amplification at the receiving coil, and to use an opamp as the preamplifier. For experimental purposes it was also desired to be able to set the quiescent level at different voltages in order to test various types of detecting circuits. For these reasons the LF351 was selected. The preamplifier and amplifier circuits are identical and are shown in Appendix (1) and the symbolic circuit is shown in Figure 4.1.b.

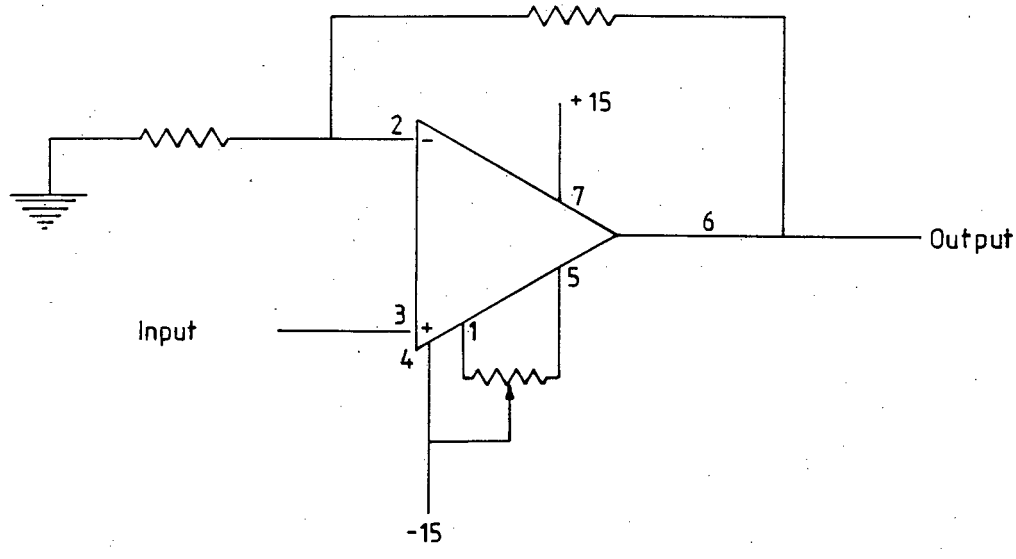

Figure 4.1.b

The quiescent voltage is set by shorting pin 3 to earth and adjusting the balance potentiometer which is connected between pins 1 and 5. The final selection of pulse shaping circuits was TTL so the quiescent level is adjusted to zero. While this adjustment proved to be quite stable, a production model would use an opamp with an earth reference. Two stages of amplification were necessary in order to get sufficient gain and prevent distortion. Other amplifiers tested included a 2N2222A transistor amplifier which produced sufficient gain in one stage but required capacitive coupling. The overall circuit with the 2N2222A proved to be noisier than the opamp.

4.2 Pulse Shaping

4.2.1 An LM339 comparator was used as a threshold detector. Since the moving coil output signal decreased as the coil moved away from the transmitting coil, the threshold had to be set to respond to the lowest positive signal. As shown in Figure 4.2.a this could be a source of error depending on how the detected pulse is used.

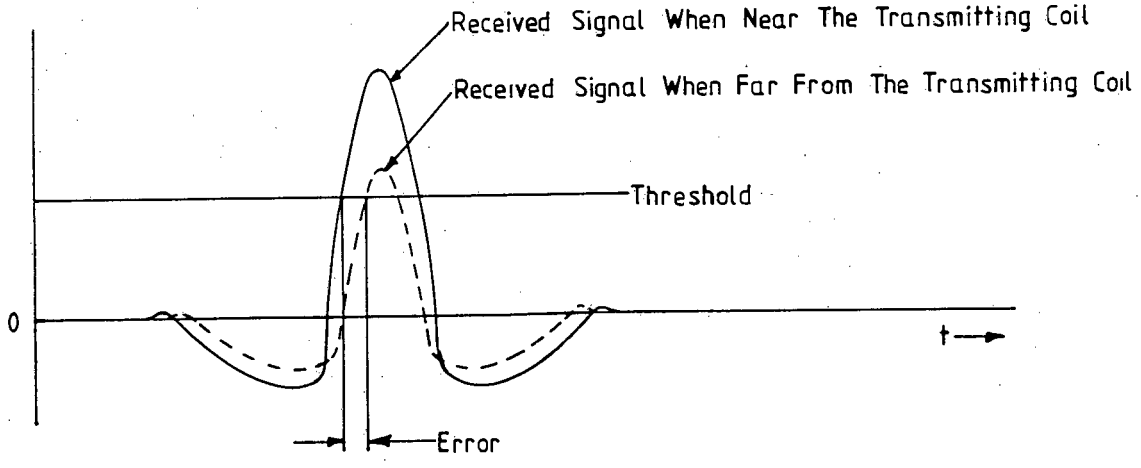

Figure 4.2.a

Error can be minimised by having a very fast rising pulse leading edge and by setting the threshhold as low as possible. In practice, the maximum error detected over 3 meters was 2 counts in 6950 (10MHz clock) which is about 0.03%. This low error is principally due to an essentially noise free circuit which allowed the threshold to be set quite low. The counting circuits can also minimise this error. Since the comparator output is a pulse of width equal to the input pulse width at the threshold, more sophisticated circuitry can be constructed to find the center time of the pulse and eliminate this source of error. Though in the final analysis it was not considered warranted in this application, a simple counter circuit was constructed that counted at 10MHz for the duration of the detected pulse and half this count was added to the count C_1. This eliminated the source of error but complicated the computer interface. The scheme is shown in Figure 4.2.b.

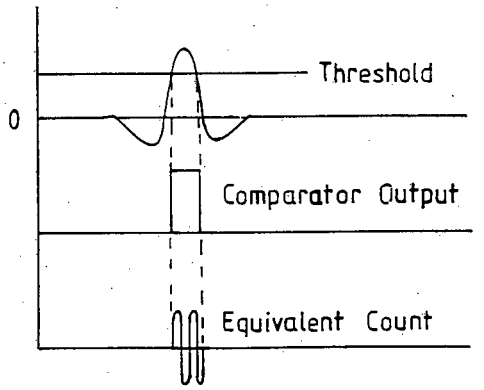

Figure 4.2.b

Since the train A count is stopped at the comparator leading edge and since both the leading edge and trailing edge of the comparator output occur at different times as

the detected input pulse height varies, adding half the variable count is equivalent to stopping train A at the center of the pulse (assuming the pulse is symmetric). The error (<1mm in 3m) is less than the calibration error and is in fact partly compensated for during calibration. Therefore, the advantage was not considered worth the complication in circuitry.

4.2.2 The output of the LM339 comparator was fed into 74LS221 monostables which triggered on the leading edge. Since the pulse traveling on the nickel wire echoed several times each transmit cycle, the output of the monostables was a series of pulses. Later circuitry was constructed to respond only to the first pulse received so this created no problem. The circuit was tested with the receiving coil output shown in 4.2.a and with a ringing pulse. As long as the first positive crossing of the ringing pulse was followed by a pulse height above the threshold, operation was satisfactory. Figure 4.2.c shows a typical ringing response. Since, for the ringing response, a large initial positive swing could not be guaranteed, the coil and circuitry to produce unsymmetrical pulses was utilised.

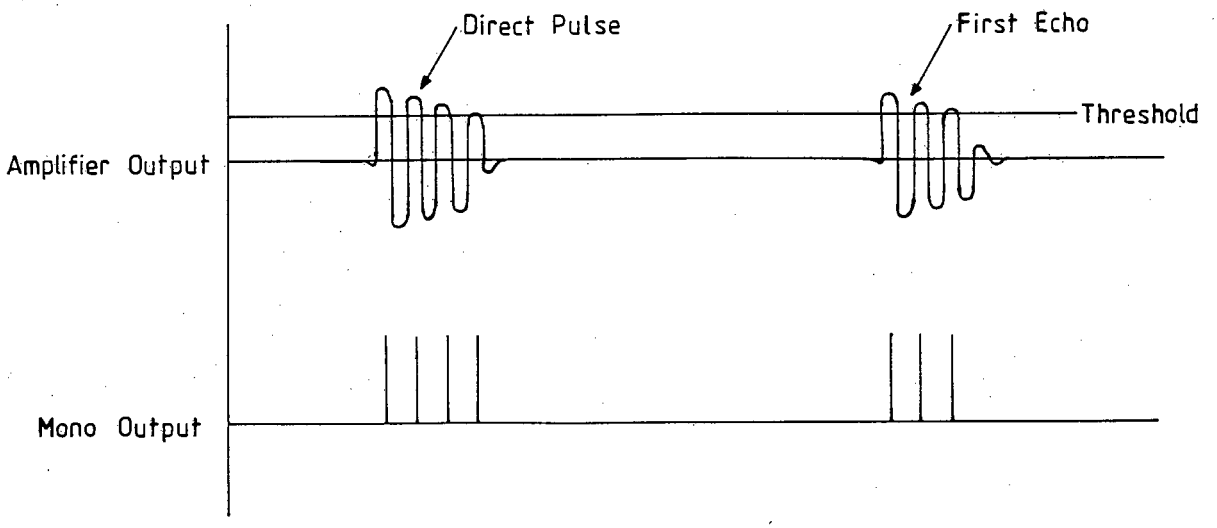

Figure 4.2.c

As the project progressed, it proved simple to discriminate against extra pulses by arranging all the timing and counting circuits to respond to the first received pulse. As a result, no attempt was made to discriminate in the pulse shaping circuits.

CHAPTER 5

TIMING

5.1 Basic Considerations

5.1.1 The optimum pulse length derived earlier was 5 microseconds representing approximately 25mm of travel. The digital pulse derived from the received pulse leading edge was stable to within 2mm (0.4 microseconds). It was decided that the maximum clock frequency usable with LS TTL logic should be used. Initially 10MHz (0.5mm resolution) was used but circuit performance justified revising this to 30MHz (0.17mm resolution).

5.1.2 The timing and counting circuits are shown in Appendix (2). The purpose of the timing circuits was to reset all circuits to an initial state, to reset the counters to zero and to start and stop the counters in response to received pulses. It was desired that the system be able to operate in a free running and a computer controlled mode. In the free running mode the computer would wait for service request (SRQ) true before reading the counters and in the computer controlled mode, the enable (pin 11) of the 74LS629 VCO would be earthed by remote enable (REN) to start a transmit cycle when the computer was ready. The pulse interval was made adjustable in the free running mode in order to accomodate various lengths of nickel wire and computer and IEEE 488 interface cycle times. Both circuits were built and tested but no advantage was found in the computer controlled version. Appendix (2) shows the free running circuitry.

5.2 Counter Control

5.2.1 The basic timing diagram is shown in Figure 5.2.a.

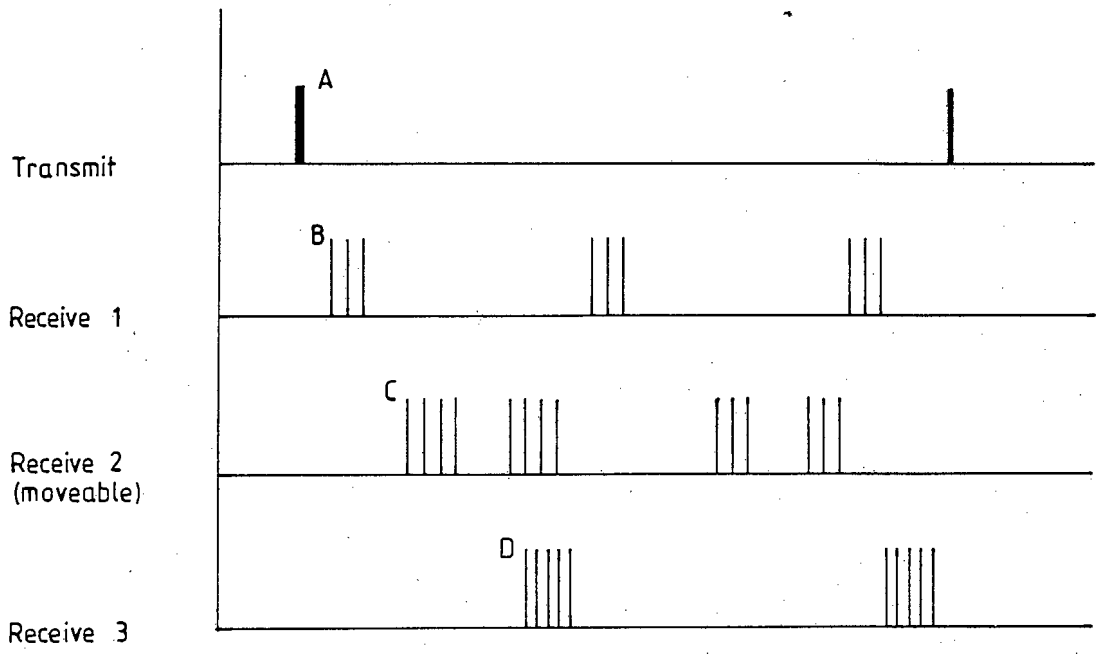

Figure 5.2.a

The sequence of events is as follows:

A. The transmitter pulses the transmit coil. At the same time the transmitter input is used to set all circuits to a starting condition and to reset both train A and B counters to zero. Approximately 3 microseconds are required in order to reset all circuits. Physically this requires a separation of about 15mm ($5mm/_{microsecond}$ x 3 microseconds) between the transmitting coil and the first fixed coil. However, it was found in practice that the transmit signal would couple magnetically to the first fixed coil if they were closer than about 40mm for a transmit pulse height of 15V and about 90mm for a pulse height of 30V.

B. The first pulse from the first fixed receiving coil arrives and starts both the A and B train counters by gating in 10MHz clock.

C. The first pulse from the moveable receiving coil arrives and stops the train A counter by gating out the 10MHz clock. This scheme was adopted because ripple counters were used and several microseconds settling time was required.

D. The first pulse from the second fixed receiving coil arrives and stops the train B counter. It also sets Service Request (SRQ) true (low) to signal the GPIB controller that a count has finished.

In the free running mode this cycle repeats with each transmit pulse. Enough time must be allowed for the computer to read both counters after SRQ becomes true and before the next transmit pulse.

5.2.2 In order to utilise a 100 meter long nickel wire and 10MHz clock, a counter capable of counting to 200,000 is required. For the experimental model the counter was constructed to allow for 3m with a 30MHz clock.

5.2.3 Since $C_1 = ft_1 = fD_1/V$ and $C_2 = ft_2 = fD_2/V$, then $C_1/C_2 = fD_1/V_1.V_2/fD_2$. Assuming that clock frequency is stable over short periods then C_1/C_2 is fixed at D_1V_2/D_2V_1. The short term drift of the crystal controlled oscillator is negligible. In several 24 hour checks of stability where temperature changed as much as 10°C from day to night the fraction C_1/C_2 did not vary more than one digit in the fourth significant digit. In the long term, f divides out. In addition any uniform changes in velocity will divide out. Several measurements were made using only C_1 as a gauge of distance to the moveable receiving coil and the effects of long term (minutes) drift and linear changes in velocity were evident. It was concluded that

the design objectives could not be met without counting the baseline and calibrating using C_1/C_2. Use of more sophisticated counters which would allow gating out a count instead of stopping the counter were investigated. Although performance was satisfactory, the savings in counter circuitry were offset by gating and holding circuitry and IEEE 488 interface control was more difficult.

5.2.4 As mentioned in Chapter 4 a counter was used to count the time equivalent to the received pulse width at the comparator threshold. This was done in order to register a count equivalent to the center of the received pulse instead of the leading edge and thereby eliminate a source of error. Since the error only occured with respect to the moveable coil only one additional set of circuits was required. This extra circuit consisted of monostables and bistables to generate start and stop pulses, the counter and reset circuitry and the circuitry to gate the count onto the GPIB. It also resulted in extra gates to produce the strobe which connected the counter to the GPIB. The extra circuits and increased cycle time were not considered justified for this application. In a commerical model they would be included.

CHAPTER 6

SYSTEM CONTROLLER AND INTERFACE

6.1 Basic Considerations

6.1.1 As a result of preceeding circuitry, counts equivalent to time t_1 and t_2 were held in two counters and a signal was generated to show that the count was completed. The minimum requirements were to detect the "count complete" signal, read the train A and B counters and use the data to either calibrate the system or read the position of the moveable receiving coil. In a commercial model of the device a microprocessor would have been used and therefore a nonstandard method of reading the counters would have been most economical. In this instance it was desired to test and experiment and a microcomputer and interface were needed. An Apple II+ was available and it was decided to try several of the IEEE 488 general purpose interface bus (GPIB) controllers, one of which was the Apple GPIB controller. However, there was no need for full implementation of a bus interface in the measuring device so ways of implementing a minimum interface were investigated. References (7), (8), (9), (10) and (11) provided all basic data needed to select the controller and design the device interface.

6.2 IEEE 488 Interface

6.2.1 The GPIB controllers investigated were full implementations of the IEEE 488 standard. They were addressable in either Applesoft basic or in machine language. The Apple GPIB controller contained a chip that was directly addressable by the computer and programming that allowed the GPIB to operate approximately ten times faster than when using Applesoft basic. In each case the minimum required communication consisted of checking the GPIB for SRQ true, addressing the device (with attendent handshake) and requesting a sequential read of each

counter stage. All data read was interpreted as ASCII characters and transmitted to the Apple II as such. While the GPIB's were capable of handling the full set (256) of ASCII characters, the Apple II could not since the eighth bit is not used in the ASCII character representation.

6.2.2 The following brief discussion assumes the reader is familiar with the IEEE 488 bus protocol. It is not essential to read this paragraph in order to understand how the device interfaces with the IEEE 488 bus. The discussion is particular to the Apple II GPIB but is very similar for the other devices. Figure 6.2.a shows the 16 bus lines as defined by the IEEE 488 standard.

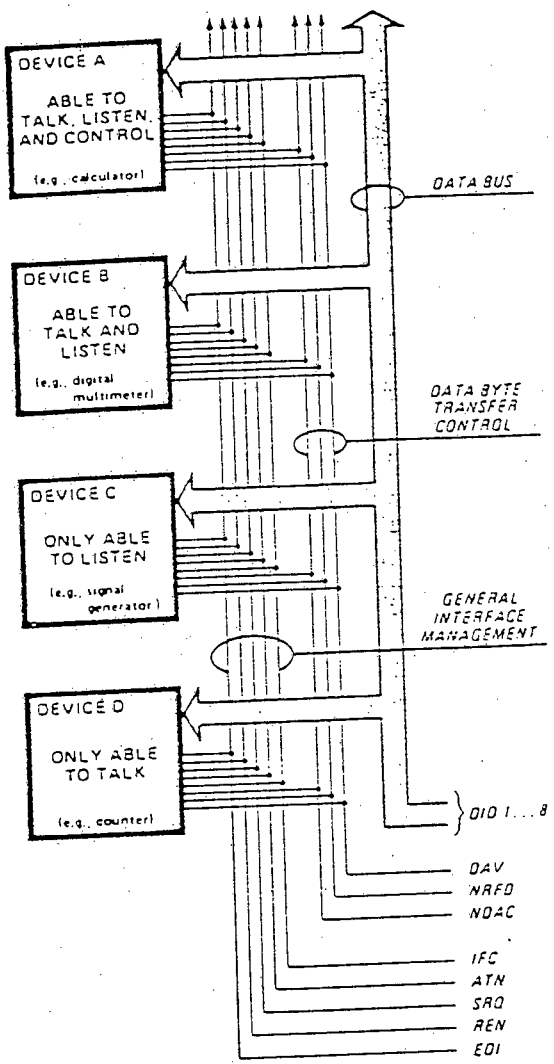

Figure 6.2.a

The Applesoft programme statement INPUT "SR"; G$ causes the GPIB controller to input T if the device is holding the SRQ line low (true) and F if it is not low (false). The computer is simply put into a loop requesting SRQ status and checking the value of G$. When G$ returns TRUE the computer starts a read routine. The programme statement PRINT "RCB"; Z$; "8"; Z$; causes the GPIB controller to sequentially read 8 ASCII characters into an 8 character string. Each data transfer occurs after an authenticated "handshake". In the Apple GPIB controller version the command mode sends three pieces of information with ATN true. As will be discussed later, the device interface was constructed to ignore the information and shake hands until ATN is false and then to send 8 characters via DIO 1-4. The 8 characters are the ASCII equivalent of the value of the 8 four bit counters. The 8 characters are read sequentially into a string and stored in Apple memory as C$. The last function in the read sequence is for the measuring device to set SRQ to false which puts the computer back into the initial loop. Just prior to entering the loop, the ASCII characters are translated to numbers, C_1 and C_2 are calculated and depending on the mode (calibrate or read) the value of position is calculated or the calibration table is filled. Several difficulties were encountered by trying to use ASCII characters as numbers. Each counter could contain a number from 0 to 15 (base 10) which corresponds to characters including null and carriage return. Attempting to translate these characters using Applesoft would not work. The problem was resolved by hard wiring DIO 5-8 lines to translate a zero reading to

character @ and then after decoding as a number simply to subtract 64 to obtain the true counter reading. Figure 6.2.b shows the ASCII character equivalent used.

DEC	OCT	HEX	CHAR	WHAT TO TYPE
64	100	40	@	@
65	101	41	A	A
66	102	42	B	B
67	103	43	C	C
68	104	44	D	D
69	105	45	E	E
70	106	46	F	F
71	107	47	G	G
72	110	48	H	H
73	111	49	I	I
74	112	4A	J	J
75	113	4B	K	K
76	114	4C	L	L
77	115	4D	M	M
78	116	4E	N	N
79	117	4F	O	O

Figure 6.2.b

As an example, if C$ = "BCDEFGAB" then the four counters of C_1 are represented by BCDE and when decoded

$$C_1 = (66-64) + 16(67-64) + 256(68-64) + 4096(69-64).$$

A similar decoding is performed for C_2. This decoding problem was unfortunate and resulted in having to gate 4 bits onto the bus at a time instead of 8 bits at a time. With 8 bits there was no simple way to translate. A look up table was prepared for the 8 bit characters but the look up time was excessive and resulted in too few measurements per second. However, the simplicity of the 4 bit system compared to one in which the measuring device would convert numbers to their ASCII equivalent before interfacing with the GPIB more than compensated for having to use 4 bit gating. In addition the "READ COUNT" command was extremely rapid and reading up to 80

characters did not substantially increase the computer/GPIB controller cycle time.

6.3 Measuring Device Interface

6.3.1 The measuring device interface consists of a circuit which can "handshake" when the bus ATN line is true and can "handshake" and gate data onto the DIO 1-4 lines when ATN is false. The interface and counters are shown in Appendix (2). Since the measuring device is the only thing on the bus, it can ignore the GPIB controller sending addresses and information and other than handshaking need only to be able to reply to the "READ WITH COUNT" request. This request does not require the end or identify (EOI) signal since it stops when the requested count of ASCII characters is received. Additionally, the timing of the IEEE standard did not have to be adhered to as long as the handshake was recognised. These factors greatly simplified interface design. The address mode handshake according to IEEE 488 is shown in Figure 6.3.a.

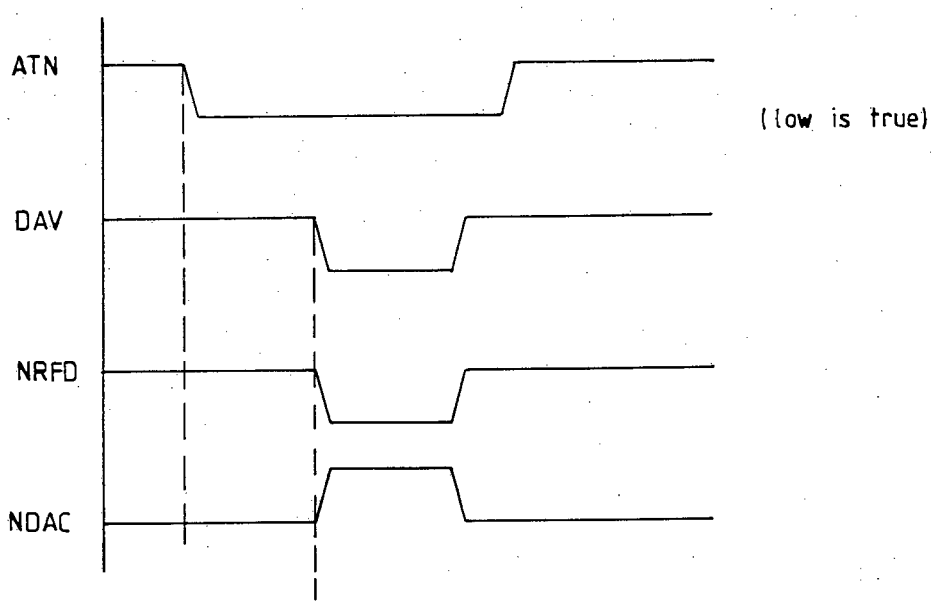

Figure 6.3.a

The only critical event is that NRFD and NDAC cannot both be high when the GPIB controller monitors their lines. If they are both high (false), the controller registers "device not present". The IEEE standard requires response to ATN within 200ns but none of the controllers monitored the lines before several microseconds had elapsed. During the address mode handshake the device must respond to the handshake in order to continue communicating but does not use any of the transmitted addressing data. During this mode the GPIB controller has control of ATN and DAV lines and the device has control of the NRFD and NDAC lines. This allowed very simple address mode handshake implementation as shown in Figure 6.3.b. NAND gates were used throughout.

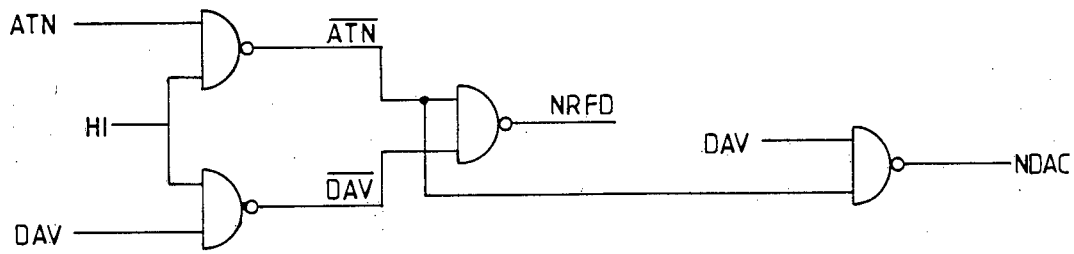

Figure 6.3.b

Before the "READ COUNT" instruction is received both ATN and DAV are high (false). This causes $\overline{ATN}$ and $\overline{DAV}$ to be low and sets NRFD and NDAC to be high. This is the quiescent state. All gates used are such that when any gate connected to the bus goes low the bus is pulled low. The READ COUNT instruction causes the controller to first address the bus as a controller and then become a

listener. During the address mode several words are placed on the bus depending on which controller is used. In this application they are simply ignored and the device continues hand shaking as long as ATN is low. When the GPIB controller addresses the bus it first pulls ATN low which makes $\overline{ATN}$ high. Since DAV is high NDAC goes low, and since $\overline{DAV}$ is low NRFD stays high. This meets the monitoring criteria that both NRFD and NDAC may not both be high when the controller monitors the bus. Shortly after the controller puts an address or command on the bus it pulls DAV low. This makes $\overline{DAV}$ high and with $\overline{ATN}$ high it makes NRFD low. At the same time DAV low makes NDAC high and the conditions for 3-wire handshake are met. Each time the controller changes addresses or commands it cycles DAV which causes the handshake routine to repeat. When ATN goes high (after the GPIB controller has finished as a talker) the handshake timing shown in Figure 6.3.c is used.

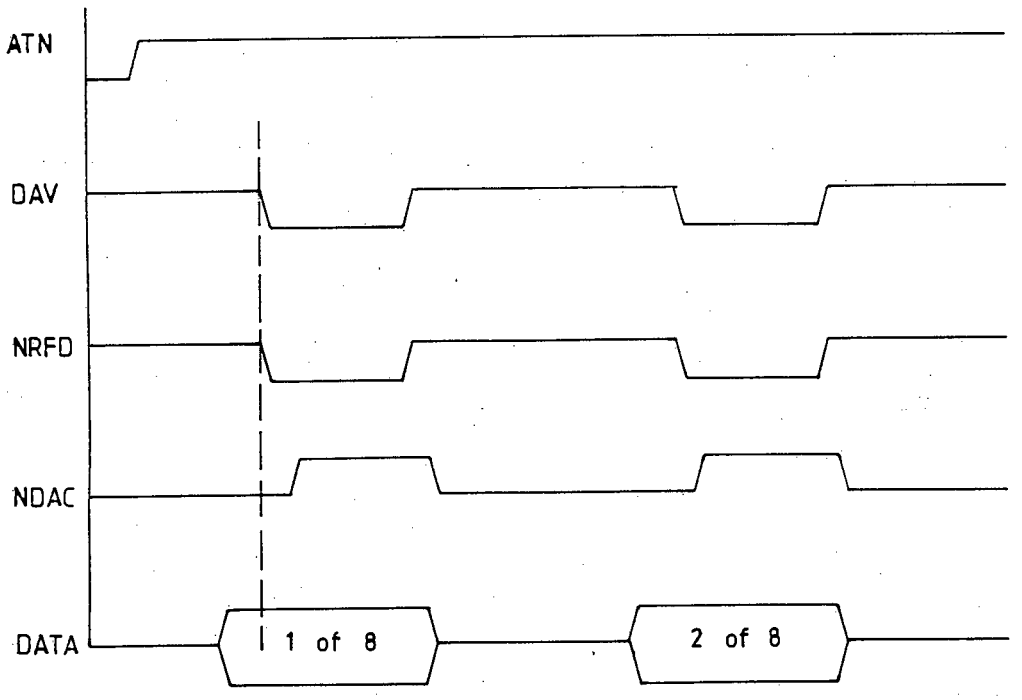

Figure 6.3.c

In this case the device must be able to shake hands, count the handshakes and strobe data on the DIO 1-4 lines. The simplified circuitry shown in Figure 6.3.d accomplishes this. Appendix (2) shows the complete circuit.

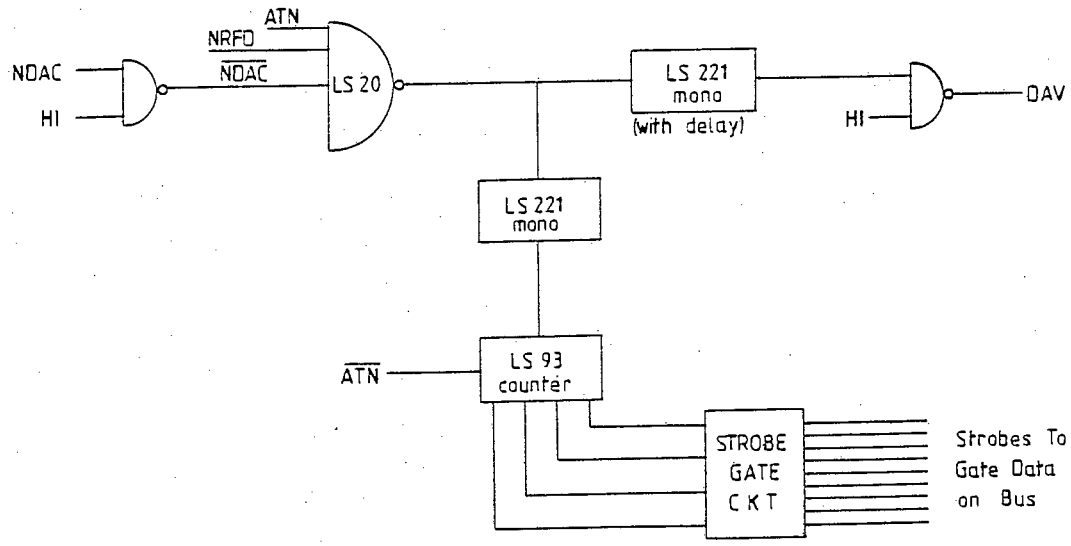

Figure 6.3.d

In the device talk mode, the device has control of DAV and the controller as listener has control of NRFD and NDAC. Three high inputs to the LS20 are required in order to get the low output. The LS221 generates pulses on the negative going edge. When ATN goes high, $\overline{ATN}$ goes low and resets the LS93 counter to all zeros. The controller sets ATN high, NRFD high and NDAC low in order to get ready for data. This makes all the inputs to the LS20 high and gives a low output. The first LS221 triggers on the negative going edge and causes the LS93 to count. 0001 out of the LS93 strobes the data from the first counter

in train A onto the DIO 1-4 lines. After a short delay the second LS221 outputs high which pulls DAV low (true). The controller shakes hands and reads the data. The short delay ensures data has settled on the bus. The width of the second LS221 pulse is sufficient to keep DAV low until the handshake and data read are finished. DAV low causes the controller to change the status of NRFD and NDAC which makes the output of the LS20 go high. Since the LS221's respond to the negative going edge, nothing else happens. At the end of the LS221 pulse, DAV goes high which causes the controller to change the status of NRFD and NDAC. This generates the next negative pulse from the LS20 and the cycle repeats, this time with a counter output of 0010 which gates the second train A counter onto the bus. The measuring device does not check that the handshake is correct but simply uses the controller ATN, NRFD and NDAC signals to operate its circuitry. If the controller responds incorrectly, the system will not work. Proper response is very simple to check. This cycle can be repeated any number of times up to the maximim (80) allowed by the controller. In practice the "READ COUNT" instruction terminates controller response when the correct number of characters (8 in this case) have been read into C$. The variable delay and pulse width of the LS221 that controls DAV allow timing to meet the requirements of any of the GPIB controllers including ones that respond exactly to the IEEE 488 standard.

6.3.2 The original scheme to save on interface circuitry was to have the controller transmit the ASCII character which corresponded to each 4-bit counter output and then translate the characters to the equivalent number. The 4-bit counter could register any number (base 10) from 0

to 15. These numbers correspond to various punctuation, symbols and control characters used by the Apple II. The Applesoft basic function ASC will not translate several of these symbols and control characters. Since DIO 5-8 were not needed for data transfer and since the device did not respond to the addresses or commands, the bus was hard wired to make the smallest number 40H. This way all counter output values could be decoded using the basic function ASC and subtracting 64.

CHAPTER 7

CALIBRATION

7.1 Basic Considerations

7.1.1 It was desired to have the device able to be calibrated in place with no extra equipment except a bench mark and scale. Calibration was to be able to compensate for temperature and tension changes as well as non-linear effects. As explained in Chapter (1) it is possible to remove linear effects on pulse velocity by calibrating to an equation of the type $D = K_1 C_1/C_2 + K_2$ where C_1 and C_2 are the counts for the variable distance and the fixed baseline respectively.

7.2 Calibration

7.2.1 Calibration was effected by a programme that sequentially read in values of C_1, C_2 and input the position of the moveable receiving coil. The device had been built on an old optical test bench and this proved ideal for calibration and experimentation. The optical bench had a scale attached to the bed plate and a pointer on the moveable trolley to which the receiving coil was fixed. It was possible to read scale values to within about $\pm$ 1mm. The values of the three variables were stored in a text file (maximum 50 values) and also printed out as a permanent record. After all calibration data points were in, a regression was performed and the values of K_1 and K_2 calculated. The values of C_1, C_2, D (position) and error in position were printed out and also stored in another text file. This data was available for plotting. In general, the only plot of interest is the error plot. Reference (12) was the source of all regressions used. The linear regression was used to fit the calibration data to a straight line. The other regressions were used in an attempt to model the calibration errors.

7.2.2 Hundreds of calibrations were performed under varying conditions of temperature, nickel wire stress, nickel wire annealing and cold working and nickel wire magnetisation. As predicted, uniform changes had essentially no effect on calibration values. Of considerable interest was the fact that the calibration data were perfectly repeatable provided non-uniform changes had not been made to the wire. Figure 7.2.a shows repeatability under worst case conditions. As shown in Chapter 8, stretching the wire removes most errors. Appendix (3) shows typical calibration error curves. Several methods were used to reduce the calibration error to a minimum. The first was to fit the error data to an nth order curve and to subtract the error curve value from the corresponding reading. The next method was to tabulate the error curve values and to subtract a linearly extrapolated value from the reading. The third was to construct a linear fit in a piecewise fashion. All methods worked well enough but it was found that by carefully stretching the wire to achieve uniform properties, the error could be reduced to $\pm$ 2mm maximum.

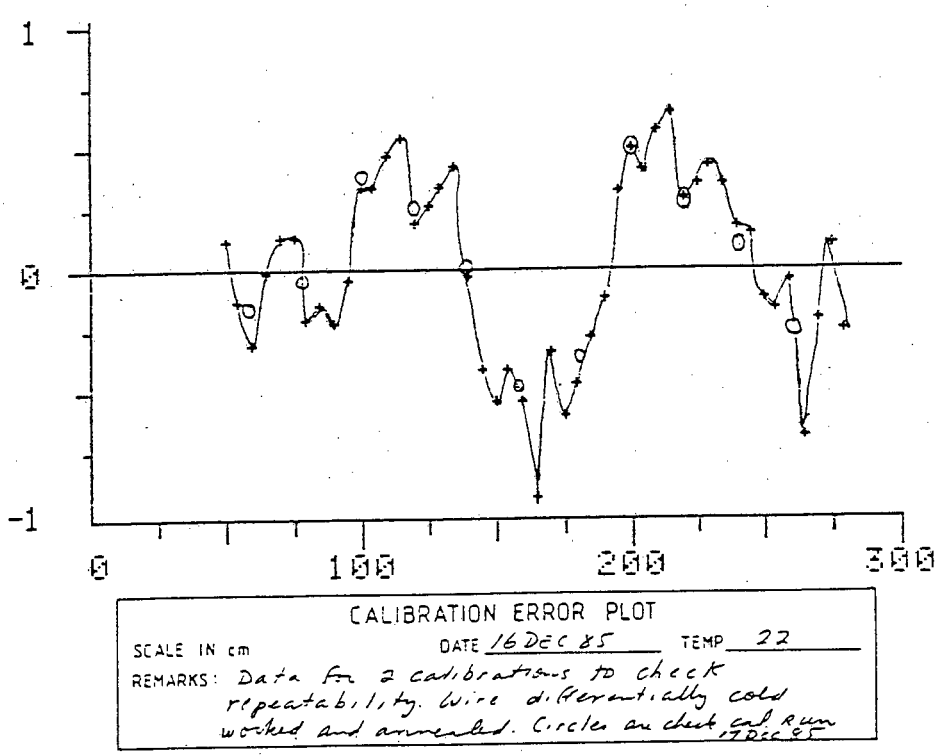

Figure 7.2.a

Page 2 of 3

X(MEAS)	C1/C2	X(CALC)	XERR
30	.0888119954	30.3829976	-.38299761
40	.122313573	40.7987091	-.79870908
50	.153324679	50.4401277	-.440127671
60	.184218119	60.0449637	-.044963643
70	.216274708	70.0114251	-.0114250779
80	.249026115	80.193907	-.193906963
90	.278643579	89.4020393	.59796077
100	.312265512	99.8551695	.144830555
110	.344349834	109.830253	.169746757
120	.375324675	119.460397	.539603084
130	.406926407	129.285442	.714557588
140	.4404676	139.71347	.286529601
150	.473661423	150.0335	-.0335003138
160	.505484988	159.927514	.0724859238
170	.53767321	169.934901	.0650994778
180	.57130485	180.391049	-.39104867
190	.600317552	189.411159	.588840723
200	.634237875	199.95706	.0429404974
210	.66671478	210.054198	-.0541981459
220	.698426447	219.913423	.0865774155
230	.729897503	229.697841	.302159309
240	.76284642	239.941729	.0582712889
250	.795612009	250.12862	-.12861985
260	.827342284	259.99363	6.37042523E-03
270	.861576213	270.637031	-.637030721
280	.893491124	280.559444	-.559444189

COEFF OF DETERM.=.999974963

COEFF OF CORREL.=.999987481

STD ERROR OF ESTIMATE=1.25636617E-03

Y(CALC)=-8.91328764E-03+(3.21644639E-03*X)

X(CALC)=2.77116002+310.90212C1/C2

RUN #1
4 JAN 86

Figure 7.2.b
TYPICAL CALIBRATION DATA

7.2.3 Many reading runs were taken for extended periods (10-12 hrs) with the moveable coil locked in position. The temperature was recorded at each half hourly reading. While there were small long term oscillator drifts, the quotient C_1/C_2 was essentially constant even though ambient temperature was changed by almost 10 degrees. No attempt was made to quantify the results inasmuch as the tension changes due to wire and optical bench changes were not known. It was beyond the scope of this thesis to instrument the nickel wire in order to measure tension directly. Typical results are tabulated in Appendix (3).

CHAPTER 8

RESULTS OF SOME EXPERIMENTATION

8.1 Changes in Parameters Affecting the Wire

8.1.1 While wire tension was not measured directly, a series of checks was made of the effects of tension changes. The decrease in loss and increase in difficulty of launching a signal were well quantified in the literature so a quick check was made to ensure that the measuring device did not suffer from some anomalous behavior. Tension was increased in steps and checked by vibrating the wire and measuring the vibratory frequency. Received pulse height, pulse height decrement and number of echos were recorded. No anomalous behaviour was noted. Cold working the wire by stretching and then releasing to a tension where good signal reception was obtained resulted in a much smoother calibration curve with smaller errors. This indicates that suitable treatment of the wire improves uniformity of velocity along the wire. In fact, the improved performance was such that annealing was not required. Figures 8.1.a and 8.1.b show the results of calibration with non-uniform conditions and after stretching.

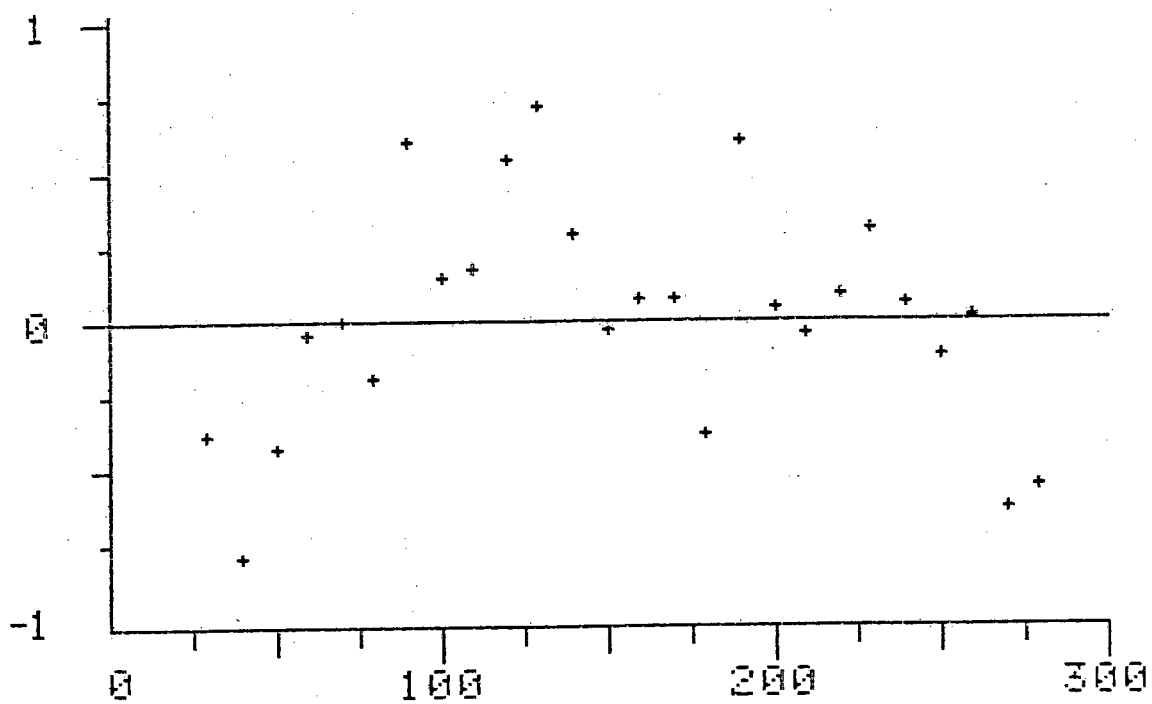

Figure 8.1.a

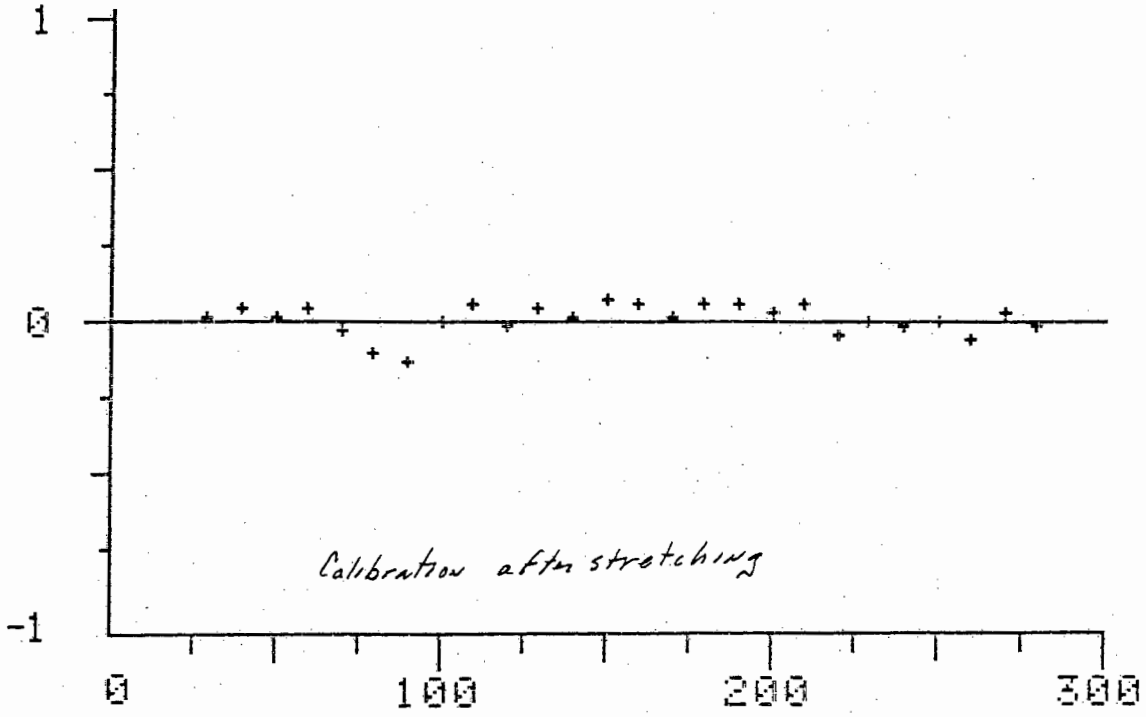

Figure 8.1.b

8.1.2 The nickel wire was magnetised along its length in one direction, the system was calibrated and then the wire remagnetised along its length in the opposite direction, and a second calibration performed. The maximum effect was achieved when the magnetisation was in the opposite direction. A marked decrease in received signal strength was noted and the values of C_1, C_2 and the calibration constants changed slightly. In one position, the moveable receiving coil did not provide enough signal to reach the comparator threshold and the system failed to work. The effect was identical to reducing the bias magnet strength by placing another magnet near the receiving coil bias magnets. It is concluded that system performance would be degraded in the presence of strong magnetic fields. The effect could be partly mitigated by shielding the receiving coil bias magnets, or by making the bias magnet field strength larger. Figure 8.1.c and 8.1.d show the calibration curves for magnetised wire.

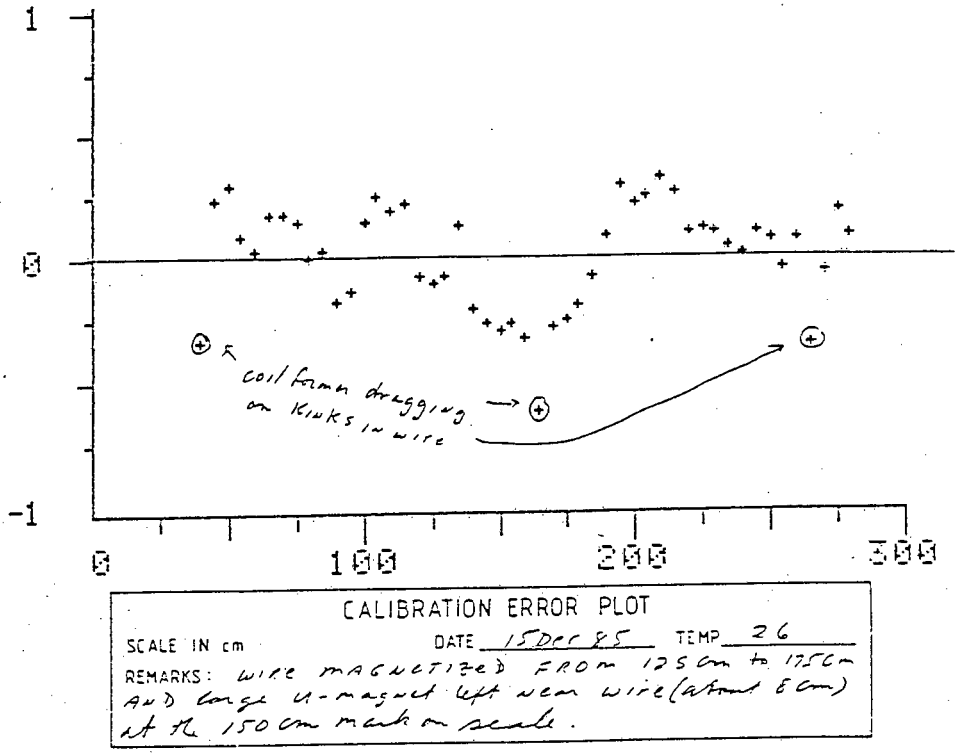

Figure 8.1.c

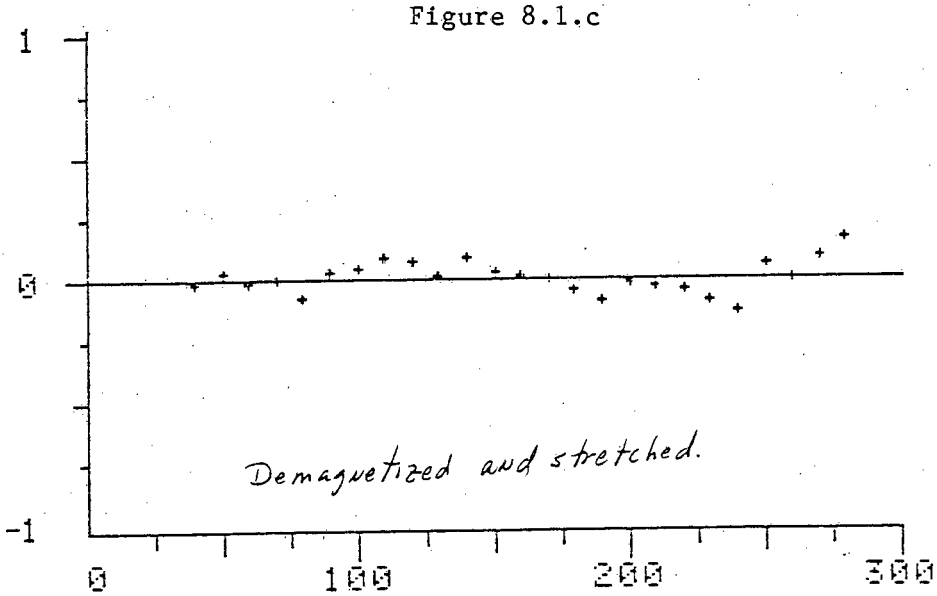

Figure 8.1.d

8.1.3 The nickel wire was heated at discrete locations and the system calibrated. This heating produced large changes in the calibration values and the errors are plainly visible in the calibration data shown in Appendix (3). The wire

was supplied in a cold drawn condition and was annealed in an open flame. The resulting abrupt changes in sound velocity cause large distortions in the calibration error curve. Subsequent stretching returned the wire to a uniform condition and calibration data returned to nominal. Figures 8.1.a and 8.1.b show these effects.

8.1.4 The nickel wire was preferentially cold worked by repeated bending and straightening. This produced the same effects as discussed in paragraph 8.1.3 and the effects were removed as before by stretching.

8.2 Changes in Counter Input Frequency

8.2.1 The system was calibrated and operated at 10MHz, 20MHz, 30MHz and 42MHz. Operation at 10, 20 and 30MHz was normal. 42MHz was the limit at which the LS logic gating and counting circuits would operate. The calibration curves were identical for each frequency. However, theoretical resolution became smaller as frequency increased and ideally accuracy could be increased as well. With pulse detection being dependent on threshold detection of the leading positive edge, theoretical resolution could not be reached, nor could overall accuracy be improved beyond the limits imposed by detection errors. However, by adding 1/2 of the count between the leading and trailing edges of the comparator output, as discussed earlier, theoretical resolution could be reached and accuracy could be made dependent on conditions in the nickel wire. In order to benefit from frequencies higher than 10MHz, it was necessary to include extra counting and interface circuits, to anneal or stretch the wire and possibly to use some of the methods previously discussed for subtracting out errors detected by calibration. The calibration curve at 42MHz is shown in Figure 8.2.a.

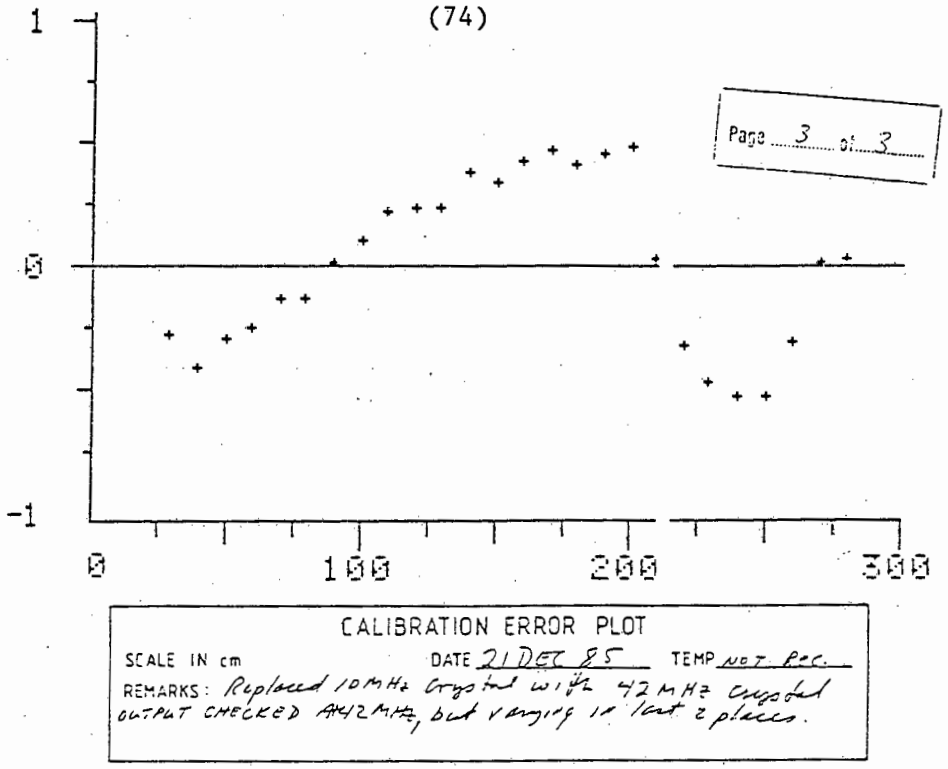

Figure 8.2.a

8.3 Changes in Detection Threshold

8.3.1 The detection circuit comparator threshold was varied from minimum to a point where the output stopped while the moveable receiving coil was fixed in position. The optical bench trolley to which the moveable coil was fixed was capable of being locked in place to prevent any coil movement. The limiting case was considered to be the end of travel at the 3 meter mark since this was the point where the pulse height was minimum and theoretically would have minimum slope. The 3 meter position should then represent maximum error due to threshold changes. The maximum difference in counts was observed to be 5 counts which is equivalent to 2.5mm. The detector threshold voltage was measured under varying conditions of supply voltage (4.5-5.5) and with the trolley at different positions. It was found to be extremely stable and the actual contribution to error was negligible. However, the change in pulse height due to

attenuation is equivalent to varying the threshold. The maximum error detected over the 3 meters due to pulse height changes was 2 counts which corresponds to 1mm. This however was not an absolute maximum error since the calibration process averages out some of the error. The error was measured by measuring the pulse height and shape at 0 meters and at 3 meters and then changing the transmitting coil bias to generate both pulses at one fixed trolley position. The count difference was the count at minimum pulse height minus the count at maximum pulse height and this corresponded to moving the trolley from 0 meters to 3 meters.

8.4 Changes in Transmitted and Received Pulse Shape

8.4.1 Several pulse shapes were generated by coupling the input to the 2N2222A transistor through differentiating and integrating circuits and by changing transmitting coil bias and position with respect to the reflecting cube. Nothing of note was observed except that the fastest rise time pulse produced the maximum receiving coil output and the minimum error. It had been surmised that improved matching between transmitter and coil could be obtained by varying the input pulse harmonic content. The optimum pulse shape proved to be a square wave input under resistive conditions and when coupled to the coil the pulse with the fastest rise time. This was achieved by parallel capacitance across the coil. The worst case was a ringing input with the first positive swing smaller than succeeding swings. Figures 8.4.a and 8.4.b show the results.

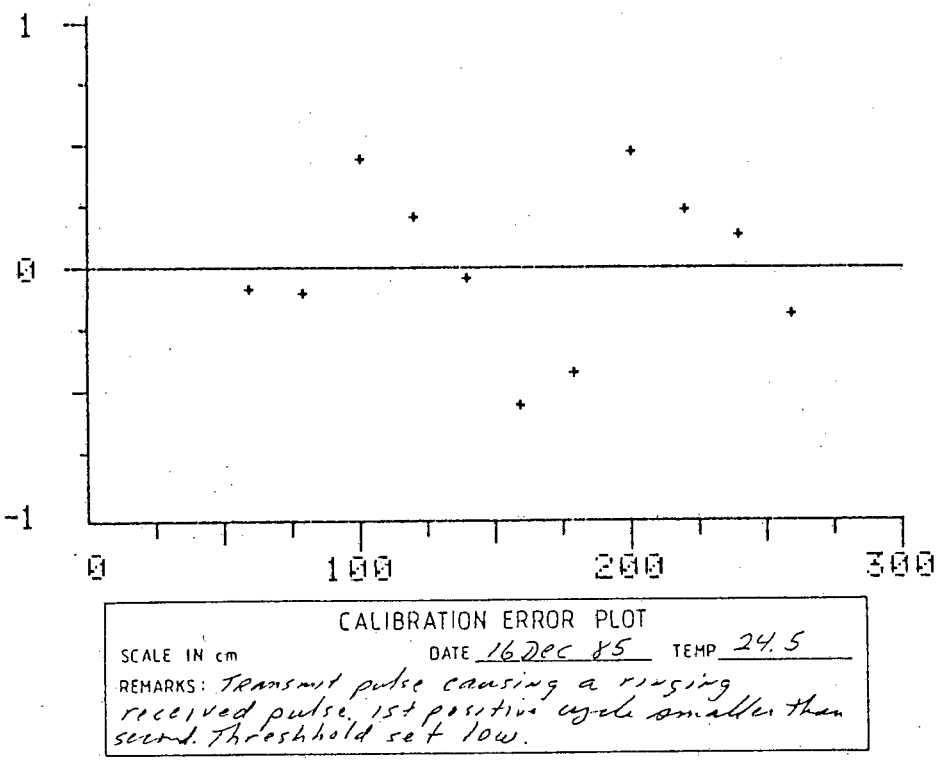

Figure 8.4.a

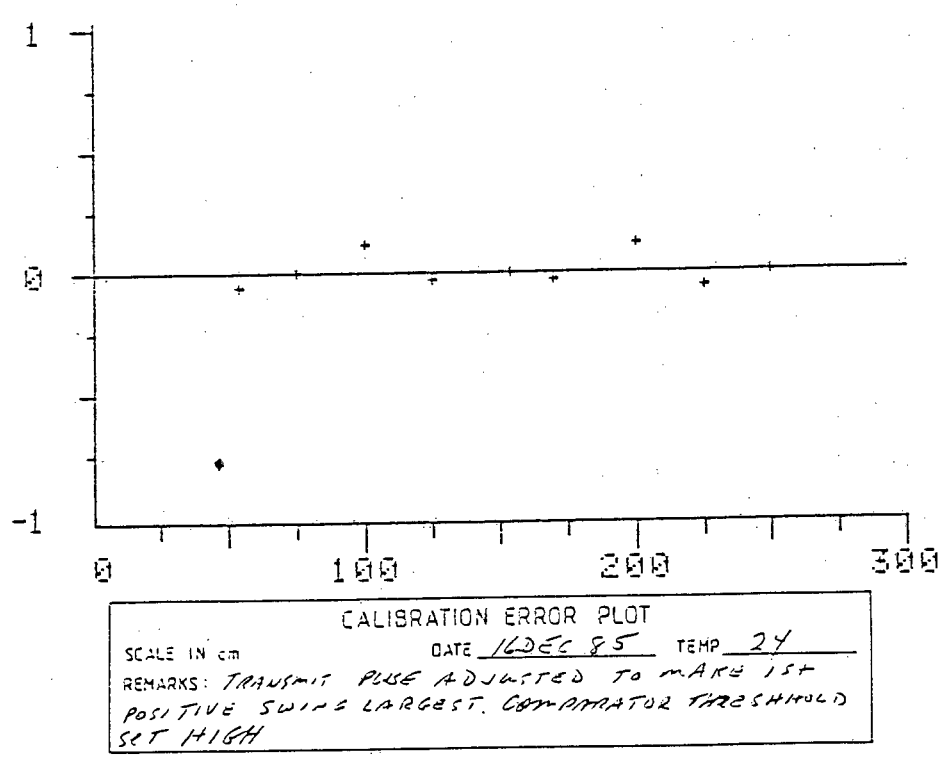

Figure 8.4.b

CHAPTER 9

CONCLUSIONS

9.1 Resolution

Near theoretical resolution was demonstrated at 10MHz. However, the physical setup was incapable of measuring resolution at 30 and 42MHz. Since resolution is directly determined by the number of millimeters per count and each clock cycle gated through was counted, near theoretical resolution should be achieved for all frequencies which LS logic will process. Small errors introduced by changing pulse height and shape due to attenuation prevented actually achieving theoretical resolution. The resolution achieved was much better than required by the intended application of the device.

9.2 Accuracy

Error was reduced to $\pm$ 1mm by making the wire properties uniform, by removing calibration error, and by using special circuits to find the midpoint of the received pulse. The goal was to obtain accuracy near to theoretical resolution. This was achieved. Theoretical resolution with the 10MHz clock is 0.5mm. However, satisfactory accuracy of $\pm$ 2.5mm was achieved by simply making the wire properties uniform by stretching.

9.3 Ability to Operate in Harsh Environments

The nickel wire loss in water was measured using a combination transmit - receive coil (from the project of Reference (1)) and a length of wire suspended in water. Then it was demonstrated that signals could be transmitted over 60 meters of submerged wire and still be detectable with the circuit of this thesis. The entire length of 3 meters of wire was cluttered with simulated swarf by attaching masking tape and by coating with petroleum jelly to which metal shavings were attached. Operation was still satisfactory. Under obscured atmospheric conditions, such as in flour mills, it is obvious that the device would work.

9.4 Calibration

Calibration for non-uniform wire characteristics was demonstrated to be extremely simple and the system was shown to be self-calibrating for conditions which changed velocity uniformly along the wire. The calibration error curve for properly treated wire (stretched and annealed) was found to be extremely repeatable and for some unexplained reason usually approximated a mathematically simple curve. While not necessary in order to meet the accuracy requirements for the uses envisaged for the device, it was nevertheless possible to reduce error by modeling the error curve.

CHAPTER 10

APPENDICES

APPENDIX 10.1

TRANSMITTING, RECEIVING AND DETECTING CIRCUITS

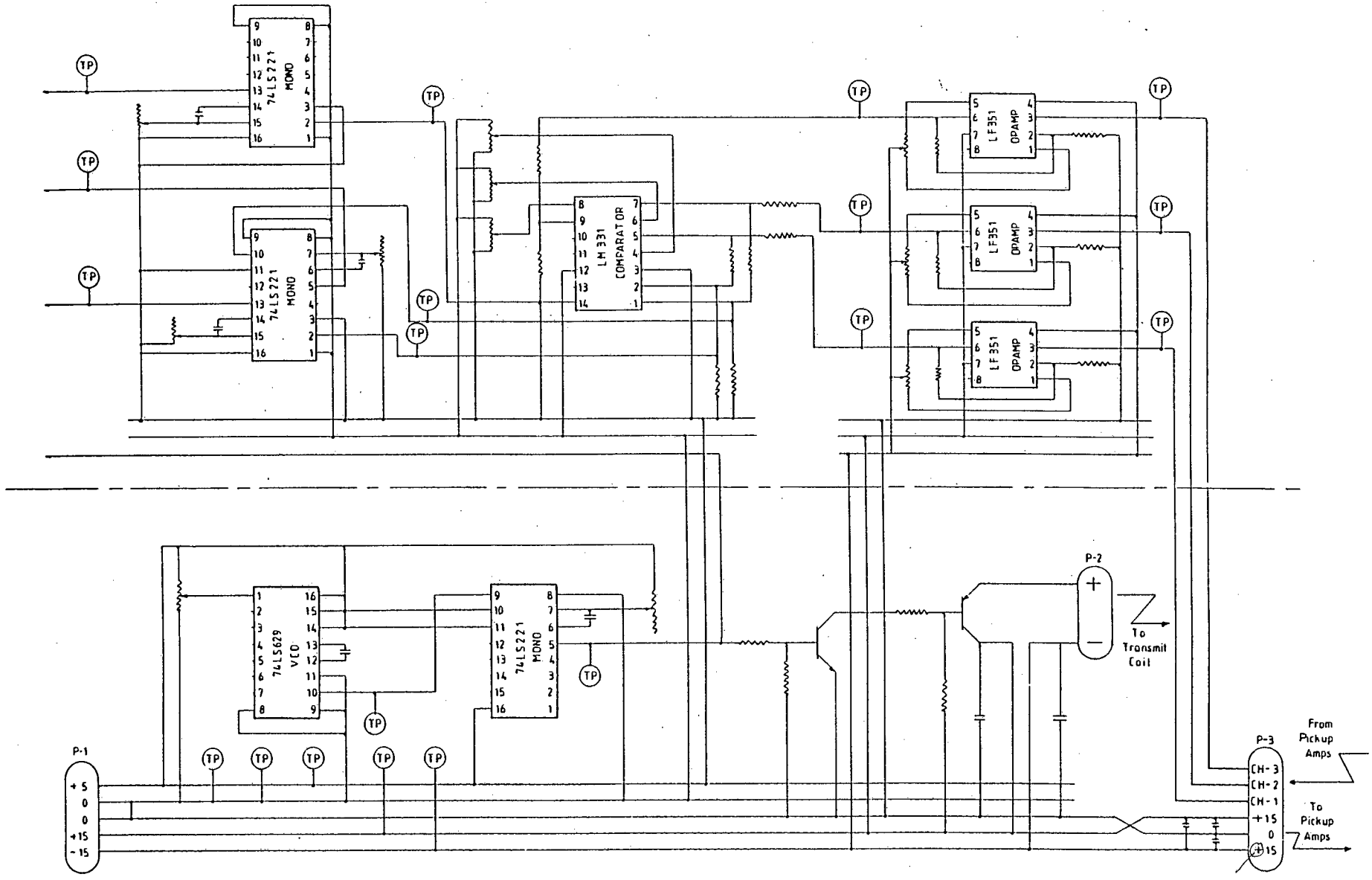
74LS221 MONO
74LS221 MONO
LM 331 COMPARATOR
LF351 OPAMP
LF351 OPAMP
LF351 OPAMP
74LS629 VCO
74LS221 MONO
TP
P-1
+5
0
0
+15
-15
P-2
To Transmit Coil
P-3
CH-3
CH-2
CH-1
+15
0
-15
From Pickup Amps
To Pickup Amps

APPENDIX 10.2

COUNTING, TIMING AND INTERFACE CIRCUITS

PLUG
GND
+5VDC
RESET
CH-1
CH-2
CH-3
74LS629 VCO
IEEE 488
PLUG
DIO-1
DIO-2
DIO-3
DIO-4
EOI
DAV
NRFD
NDAC
IFC
SRQ
ATN
SHIELD
DIO-5
DIO-6
DIO-7
DIO-8
REN
GND
PLUG
74LD1
LS 74 F F
LS 74 F F
LS 20 NAND GATE
LS 93
LS 224
LS93
LS93
LS 224

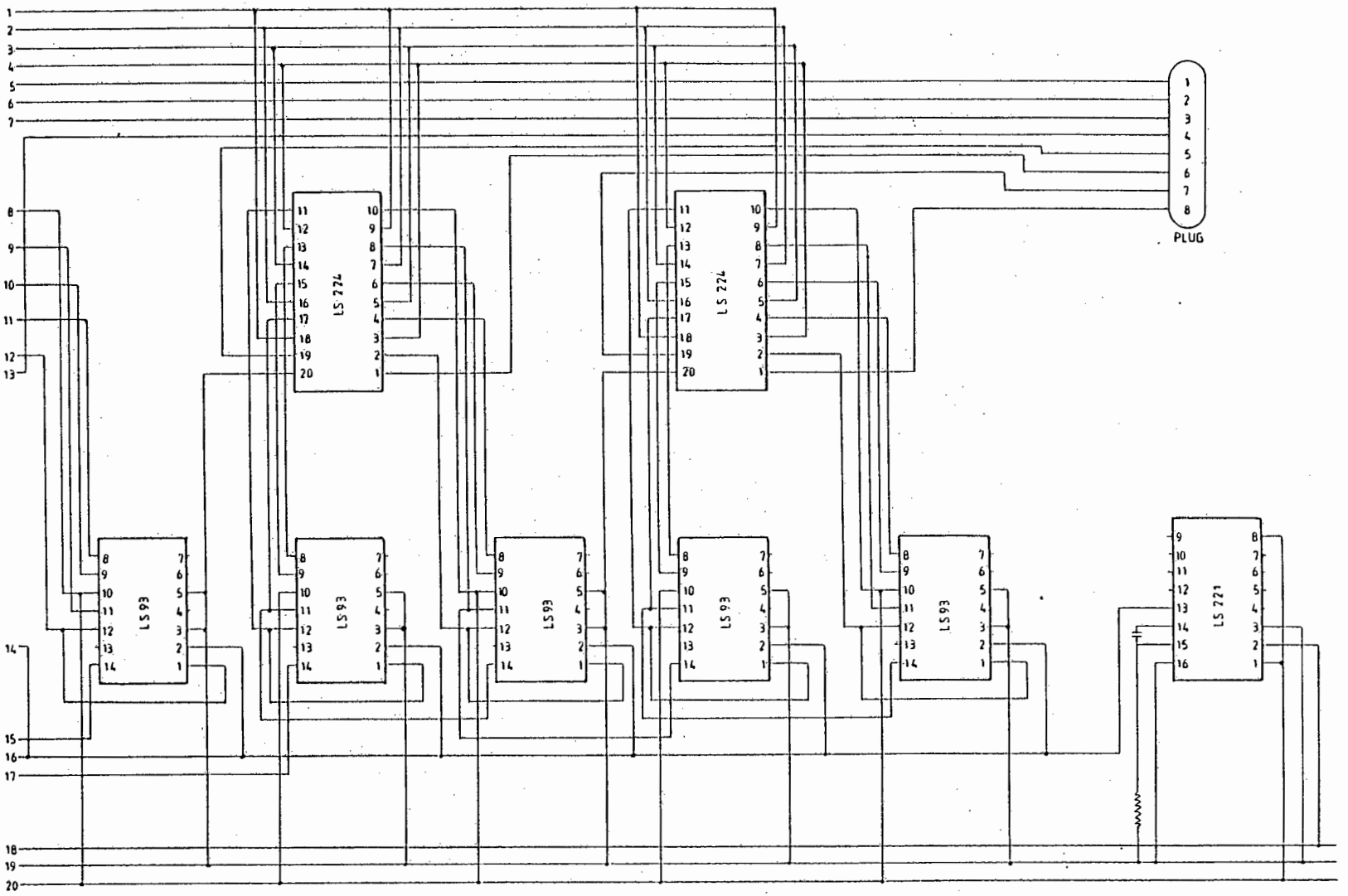
PLUG
LS 274
LS 274
LS 93
LS 93
LS 93
LS 93
LS 93
LS 221

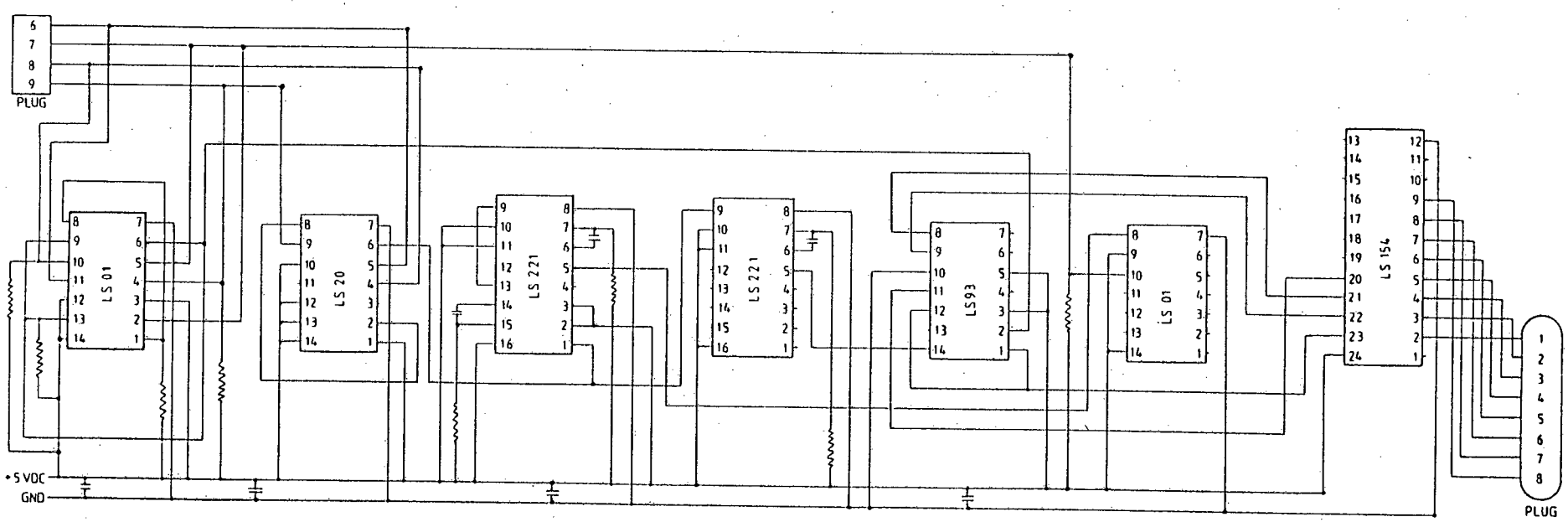
6
7
8
9
PLUG
LS 01
LS 20
LS 221
LS 221
LS93
LS 01
LS 154
+5 VDC
GND
1
2
3
4
5
6
7
8
PLUG

APPENDIX 10.3

CALIBRATION DATA

#	X	C1	C2	C1/C2
1	30	616	6936	.0888119954
2	40	848	6933	.122313573
3	50	1063	6933	.153324679
4	60	1277	6932	.184218119
5	70	1499	6931	.216274708
6	80	1726	6931	.249026115
7	90	1931	6930	.278643579
8	100	2164	6930	.312265512
9	110	2386	6929	.344349834
10	120	2601	6930	.375324675
11	130	2820	6930	.406926407
12	140	3052	6929	.4404676
13	150	3282	6929	.473661423
14	160	3502	6928	.505484988
15	170	3725	6928	.53767321
16	180	3958	6928	.57130485
17	190	4159	6928	.600317552
18	200	4394	6928	.634237875
19	210	4619	6928	.66671478
20	220	4838	6927	.698426447
21	230	5056	6927	.729897502
22	240	5285	6928	.76284642
23	250	5512	6928	.795612009
24	260	5731	6927	.827342284
25	270	5969	6928	.861576212
26	280	6191	6929	.893491124

RUN #1
4 JAN 86

X(MEAS)	C1/C2	X(CALC)	XERR
30	.0888119954	30.3829976	-.38299761
40	.122313573	40.7987091	-.79870908
50	.153324679	50.4401277	-.440127671
60	.184218119	60.0449637	-.044963643
70	.216274708	70.0114251	-.0114250779
80	.249026115	80.193907	-.193906963
90	.278643579	89.4020393	.59796077
100	.312265512	99.8551695	.144830555
110	.344349834	109.830253	.169746757
120	.375324675	119.460397	.539603084
130	.406926407	129.285442	.714557588
140	.4404676	139.71347	.286529601
150	.473661423	150.0335	-.0335003138
160	.505484988	159.927514	.0724859238
170	.53767321	169.934901	.0650994778
180	.57130485	180.391049	-.39104867
190	.600317552	189.411159	.588840723
200	.634237875	199.95706	.0429404974
210	.66671478	210.054198	-.0541981459
220	.698426447	219.913423	.0865774155
230	.729897503	229.697841	.302159309
240	.76284642	239.941729	.0582712889
250	.795612009	250.12862	-.12861985
260	.827342284	259.99363	6.37042523E-03
270	.861576213	270.637031	-.637030721
280	.893491124	280.559444	-.559444189

COEFF OF DETERM.=.999974963

COEFF OF CORREL.=.999987481

STD ERROR OF ESTIMATE=1.25636617E-03

Y(CALC)=-8.91328764E-03+(3.21644639E-03*X)

X(CALC)=2.77116002+310.90212C1/C2

RUN #1
4 JAN 86

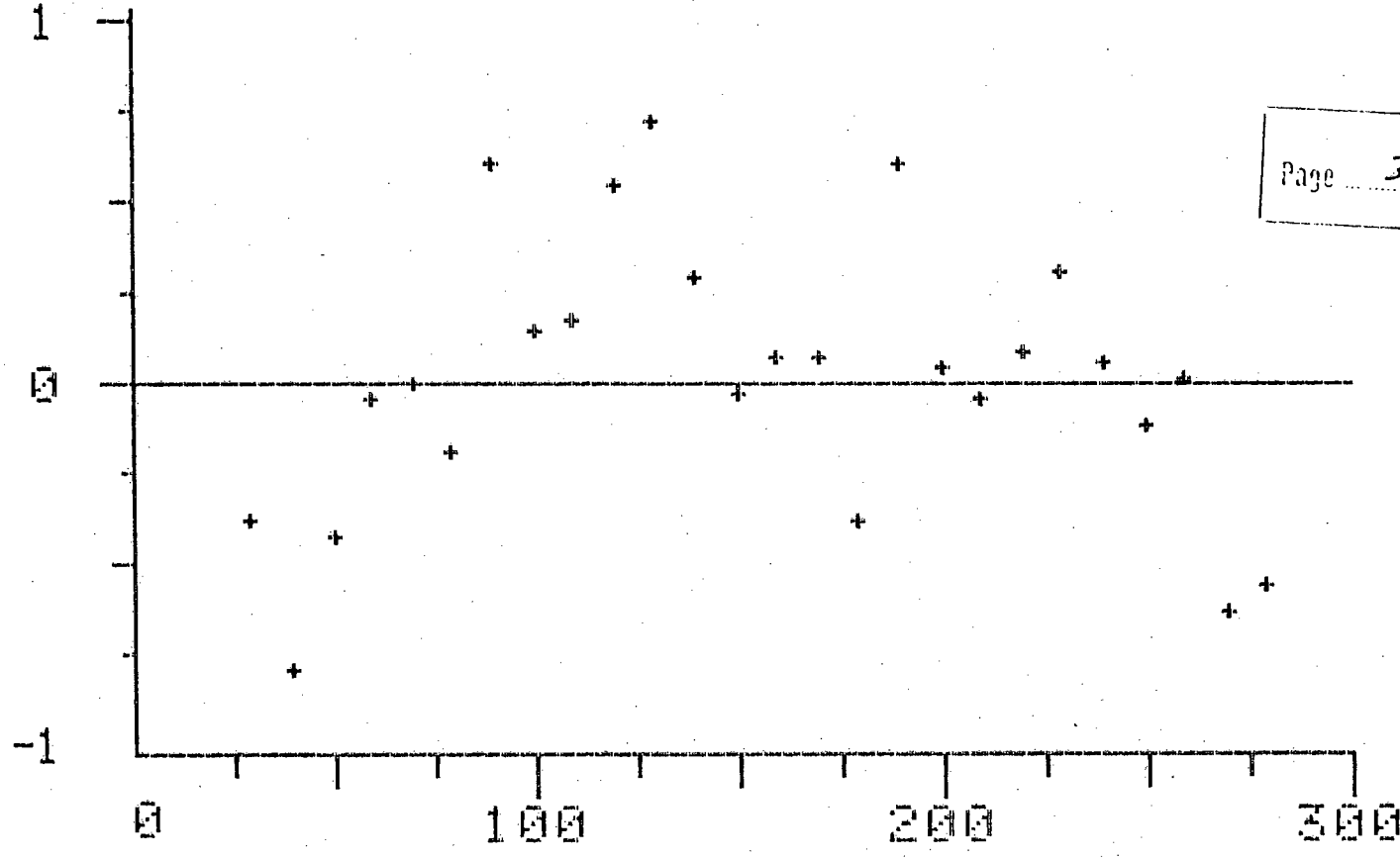

CALIBRATION ERROR PLOT

SCALE IN cm DATE 4JAN86 TEMP 24.5

REMARKS: WIRE SUBJECTED TO COLD WORKING AND ANNEALING OVER SHORT LENGTHS OF ABOUT 10 cm THROUGHOUT LENGTH OF WIRE.

#	X	C1	C2	C1/C2
1	30	494	6877	.0718336484
2	40	717	6877	.104260579
3	50	941	6877	.136832921
4	60	1164	6877	.169259852
5	70	1389	6877	.201977607
6	80	1614	6876	.234729494
7	90	1838	6876	.267306574
8	100	2059	6878	.299360279
9	110	2281	6877	.331685328
10	120	2506	6877	.364403083
11	130	2728	6876	.396742292
12	140	2952	6876	.429319372
13	150	3174	6876	.461605585
14	160	3399	6878	.494184356
15	170	3623	6877	.526828559
16	180	3845	6876	.55919139
17	190	4069	6877	.59168242
18	200	4293	6877	.624254762
19	210	4516	6877	.656681693
20	220	4741	6876	.689499709
21	230	4964	6877	.721826378
22	240	5188	6877	.75439872
23	250	5412	6878	.786856644
24	260	5636	6877	.819543406
25	270	5859	6879	.851722634
26	280	6082	6877	.884397266

RUN #2
4JAN86

X(MEAS)	C1/C2	X(CALC)	XERR
30	.0718336484	29.987744	.012255989
40	.104260579	39.9660413	.0339587033
50	.136832921	49.989084	.0109159648
60	.169259852	59.9673815	.0326185524
70	.201977607	70.0351702	-.0351701677
80	.234729494	80.1134619	-.113461822
90	.267306574	90.1379625	-.13796252
100	.299360279	100.001412	-1.41224265E-03
110	.331685328	109.948359	.051641196
120	.364403083	120.016148	-.0161475539
130	.396742292	129.967451	.0325485468
140	.429319372	139.991952	8.04781914E-03
150	.461605585	149.926948	.0730516911
160	.494184356	159.951969	.0480307341
170	.526828559	169.997125	2.87503004E-03
180	.55919139	179.955698	.0443022847
190	.59168242	189.953719	.0462805629
200	.624254762	199.976762	.0232377648
210	.656681693	209.955059	.0449404717
220	.689499709	220.0537	-.0537002683
230	.721826378	230.001146	-1.14554167E-03
240	.75439872	240.024188	-.0241882205
250	.786856644	250.012023	-.0120226741
260	.819543406	260.070274	-.0702742338
270	.851722634	269.97235	.0276505947
280	.884397266	280.026869	-.0268685818

COEFF OF DETERM.=.999999558

COEFF OF CORREL.=.999999779

STD ERROR OF ESTIMATE=1.68653917E-04

Y(CALC)=-.0256188996+(3.24974589E-03*X)

X(CALC)=7.8833547+307.716367C1/C2

RUN #2
4JAN86

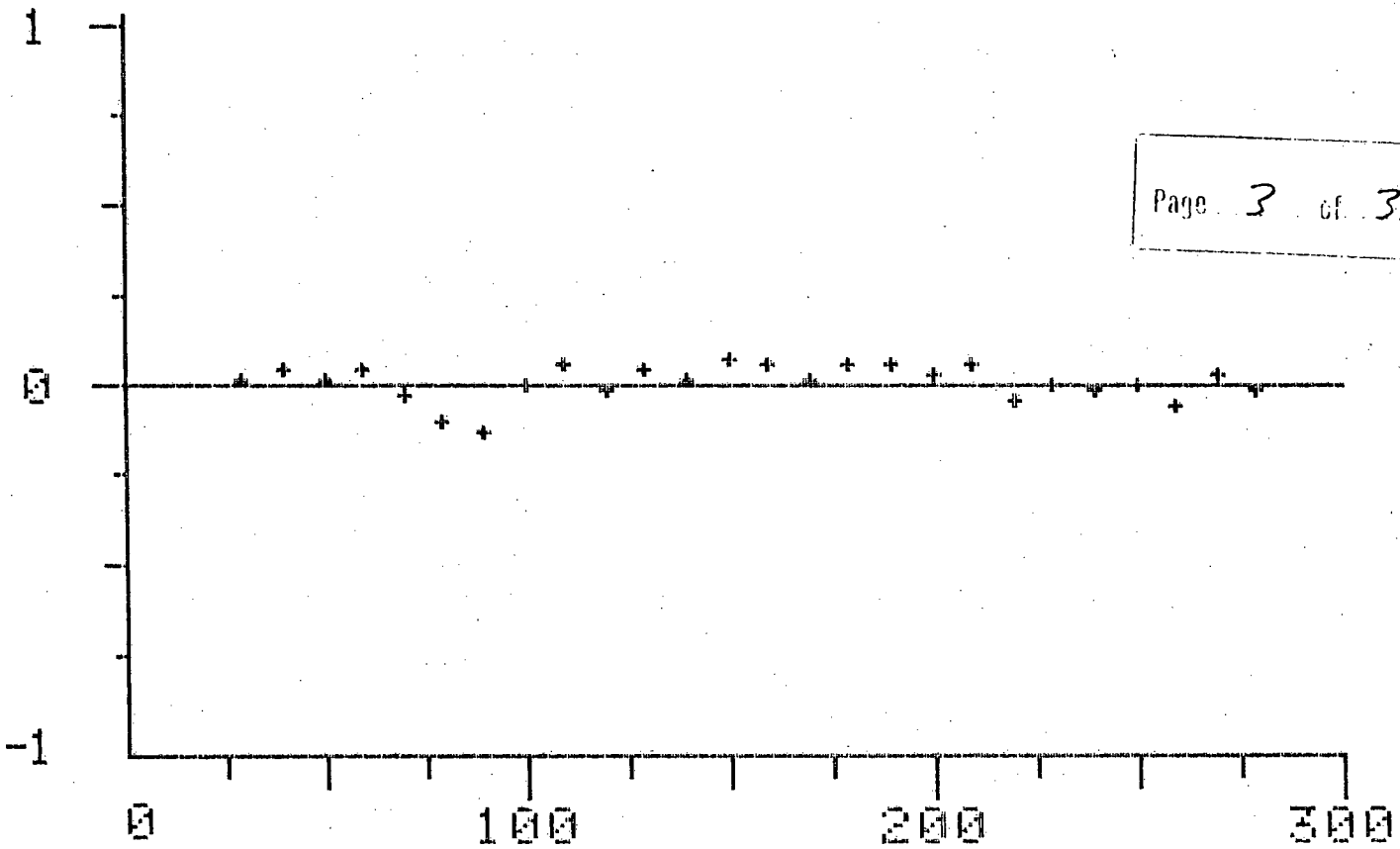

CALIBRATION ERROR PLOT

SCALE IN cm DATE 4JAN86 TEMP 24.5

REMARKS: Cold stretched the wire uniformly

#	X	C1	C2	C1/C2
1	40	873	9833	.0887826706
2	50	1196	9833	.121631242
3	60	1522	9833	.154784908
4	70	1846	9832	.187754272
5	80	2173	9833	.220990542
6	90	2494	9833	.253635716
7	100	2818	9833	.286585986
8	110	3140	9830	.319430315
9	120	3465	9830	.35249237
10	130	3792	9831	.385718645
11	140	4114	9831	.41847218
12	150	4440	9831	.451632591
13	160	4764	9829	.484688168
14	170	5090	9831	.517749975
15	180	5417	9833	.55090003
16	190	5741	9830	.584028484
17	200	6063	9830	.616785351
18	210	6390	9833	.649852537
19	220	6715	9833	.682904505
20	230	7040	9832	.716029292
21	240	7367	9833	.749211838
22	250	7686	9834	.781574131
23	260	8013	9835	.814743264
24	270	8334	9834	.847467968
25	280	8657	9835	.880223691

RUN #1
19 DEC 85

X(MEAS)	C1/C2	X(CALC)	XERR
40	.0887826706	40.0211571	-.0211570561
50	.121631242	49.9750188	.0249811858
60	.154784908	60.0213312	-.0213311762
70	.187754272	70.0117959	-.0117958784
80	.220990542	80.0831392	-.0831391215
90	.253635717	89.9753672	.0246328414
100	.286585986	99.9600458	.0399543047
110	.319430315	109.912622	.0873780847
120	.35249237	119.931174	.06882599
130	.385718645	129.999489	5.11467457E-04
140	.41847218	139.924552	.075447917
150	.451632591	149.972908	.0270916224
160	.484688168	159.989498	.0105025172
170	.517749975	170.007975	-7.97456503E-03
180	.55090003	180.053193	-.0531927943
190	.584028484	190.091865	-.0918652415
200	.616785351	200.017939	-.0179386735
210	.649852537	210.038046	-.0380455255
220	.682904505	220.053541	-.0535411239
230	.716029292	230.091102	-.0911023617
240	.749211838	240.146166	-.146166146
250	.781574131	249.952674	.0473256707
260	.814743264	260.003674	-3.67379189E-03
270	.847467968	269.920001	.0799992084
280	.880223691	279.845727	.154272676

COEFF OF DETERM.=.999999174

COEFF OF CORREL.=.999999587

STD ERROR OF ESTIMATE=2.2547298E-04

Y(CALC)=-.0432904749+(3.30008314E-03*X)

X(CALC)=13.1179952+303.022669C1/C2

RUN #1
19DEC85

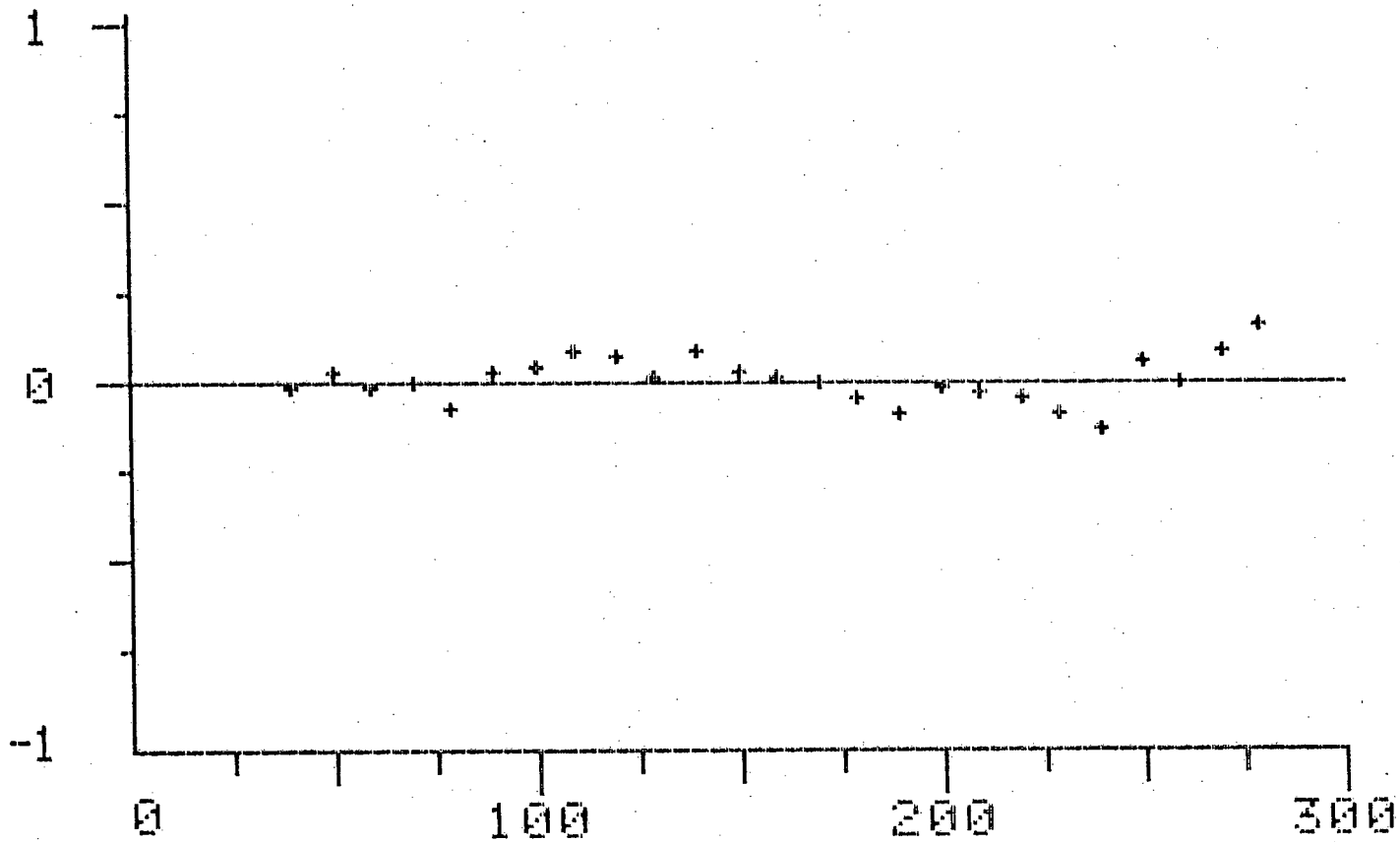

CALIBRATION ERROR PLOT

SCALE IN cm DATE 19 DEC 85 TEMP 23.5

REMARKS: 250 cm TO 300 cm MAGNETISED OPPOSITE TO PICKUP BIAS MAGNET

#	X	C1	C2	C1/C2
1	40	1051	7174	.146501255
2	45	1150	7174	.160301087
3	50	1260	7173	.17565872
4	55	1376	7173	.191830475
5	60	1489	7174	.20755506
6	65	1597	7173	.222640457
7	70	1709	7174	.238221355
8	75	1821	7174	.253833287
9	80	1936	7174	.269863396
10	85	2047	7174	.285335935
11	90	2163	7174	.301505436
12	95	2274	7175	.316933798
13	100	2379	7174	.331614162
14	105	2488	7174	.346807917
15	110	2601	7174	.362559242
16	115	2712	7174	.378031781
17	120	2830	7174	.394480067
18	125	2942	7174	.410091999
19	130	3053	7174	.425564539
20	135	3160	7174	.440479509
21	140	3279	7174	.457067187
22	145	3392	7174	.472818511
23	150	3504	7174	.488430443
24	155	3615	7174	.503902983
25	160	3728	7174	.519654307
26	165	3846	7174	.536102593
27	170	3950	7174	.550599387
28	175	4061	7174	.566071926
29	180	4171	7174	.581405074
30	185	4280	7174	.596598829
31	190	4388	7174	.611653192
32	195	4495	7174	.626568163
33	200	4608	7174	.642319487
34	205	4719	7174	.657792027
35	210	4829	7174	.673125174
36	215	4941	7173	.688833124
37	220	5057	7174	.704906607
38	225	5168	7174	.720379147
39	230	5280	7174	.735991079
40	235	5392	7173	.751707793
41	240	5505	7174	.767354335
42	245	5614	7173	.782657187
43	250	5727	7174	.798299414
44	255	5841	7174	.814190131
45	260	5950	7174	.829383886
46	265	6070	7173	.846228914
47	270	6176	7174	.860886535
48	275	6281	7173	.875644779
49	280	6395	7173	.891537711

Run #2
15 DEC 85

X(MEAS)	C1/C2	X(CALC)	XERR
40	.146501255	40.3394858	-.339485735
45	.160301087	44.7771465	.222853571
50	.17565872	49.7157546	.284245417
55	.191830475	54.9161629	.0838371217
60	.20755506	59.9727731	.0272268802
65	.222640457	64.8238374	.176162571
70	.238221355	69.8342417	.165758282
75	.253833287	74.8546258	.145374268
80	.269863396	80.0094844	-9.48441028E-03
85	.285335935	84.9850434	.0149566233
90	.301505436	90.1847269	-.184726864
95	.316933798	95.1460796	-.1460796
100	.331614162	99.866896	.133103967
105	.346807917	104.752805	.247194618
110	.362559242	109.818015	.181985497
115	.378031781	114.793573	.206426531
120	.394480067	120.082907	-.0829067826
125	.410091999	125.103291	-.103290796
130	.425564539	130.07885	-.0788500309
135	.440479509	134.87511	.124890506
140	.457067187	140.209268	-.209267676
145	.472818511	145.274476	-.274476409
150	.488430443	150.294861	-.294860482
155	.503902983	155.27042	-.270419776
160	.519654307	160.335629	-.33562851
165	.536102593	165.624962	-.624961793
170	.550599387	170.286747	-.286747038
175	.566071926	175.262306	-.262305915
180	.581405074	180.19304	-.193040371
185	.596598829	185.07895	-.0789497495
190	.611653192	189.920034	.0799657106
195	.626568163	194.716294	.28370589
200	.642319487	199.781503	.218497038
205	.657792027	204.757062	.242937803
210	.673125174	209.687796	.312203586
215	.688833124	214.739057	.260942757
220	.704906607	219.907864	.092136085
225	.720379147	224.883423	.11657691
230	.735991079	229.903807	.0961928368
235	.751707793	234.957886	.0421136618
240	.767354335	239.9894	.0105999708
245	.782657187	244.910392	.0896080136
250	.798299415	249.940518	.0594815612
255	.814190131	255.050552	-.0505518913
260	.829383886	259.936461	.0635386705
265	.846228914	265.353376	-.353376508
270	.860886535	270.066879	-.0668793917
275	.875644778	274.81274	.187260389
280	.891537711	279.923486	.0765138864

COEFF OF DETERM.=.999991277

COEFF OF CORREL.=.999995639

Run # 2
15 Dec 85

STD ERROR OF ESTIMATE=6.63101159E-04

Y(CALC)=.0210572042+(3.10970873E-03*X)

X(CALC)=6.7714394+321.573526C1/C2

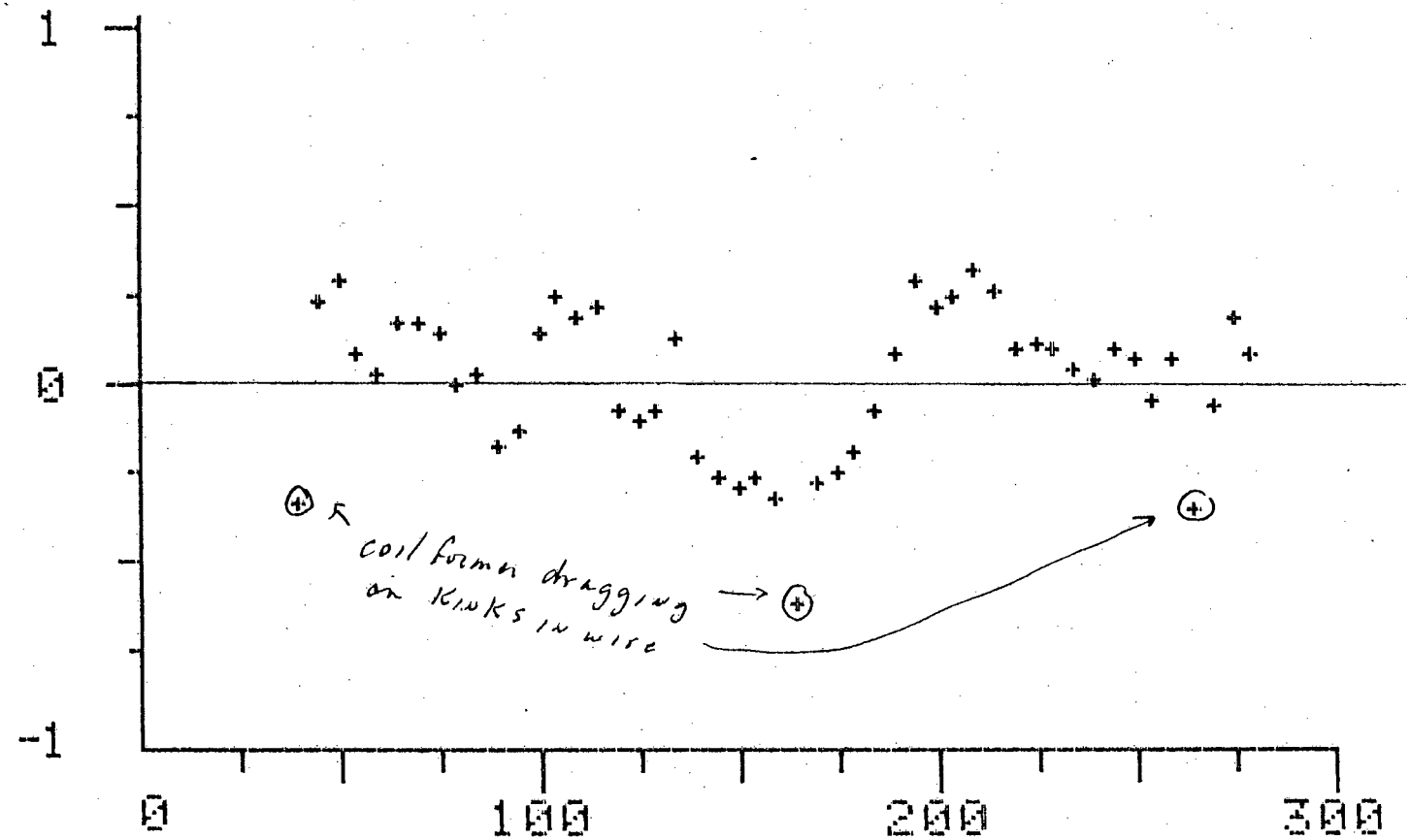

CALIBRATION ERROR PLOT

SCALE IN cm DATE 15Dec85 TEMP 26

REMARKS: wire MAGNETIZED FROM 125 cm to 175 cm AND large U-magnet left near wire (about 8 cm) at the 150 cm mark on scale.

#	X	C1	C2	C1/C2
1	30	2282	30191	.0755854394
2	40	3275	30190	.108479629
3	50	4242	30187	.140524067
4	60	5217	30185	.172834189
5	70	6184	30186	.204863182
6	80	7162	30183	.237285889
7	90	8126	30181	.269242238
8	100	9097	30181	.301414797
9	110	10066	30184	.333487941
10	120	11042	30183	.365835073
11	130	12020	30179	.398290202
12	140	12986	30181	.4302707
13	150	13967	30177	.462835935
14	160	14939	30181	.494980286
15	170	15912	30178	.527271522
16	180	16896	30176	.559915164
17	190	17871	30178	.592186361
18	200	18850	30183	.624523739
19	210	19871	30179	.658437987
20	220	20883	30177	.692017099
21	230	21878	30179	.724941184
22	240	22863	30179	.757579774
23	250	23842	30180	.789993373
24	260	24801	30182	.821714929
25	270	25756	30190	.853130175
26	280	26730	30186	.885509839

RHN #1
21 DEC 85

X(MEAS)	C1/C2	X(CALC)	XERR
30	.0755854394	30.2821254	-.282125354
40	.108479629	40.4233638	-.42336379
50	.140524067	50.3026249	-.302624881
60	.172834189	60.263796	-.263795972
70	.204863182	70.1382953	-.138295323
80	.237285889	80.1341763	-.134176254
90	.269242238	89.9862796	.013720423
100	.301414797	99.9050403	.0949597955
110	.333487941	109.793151	.206848711
120	.365835073	119.765732	.234267563
130	.398290202	129.771609	.228390932
140	.4302707	139.631157	.368842542
150	.462835935	149.67098	.329020381
160	.494980286	159.581044	.418956161
170	.527271522	169.536393	.463607609
180	.559915164	179.600387	.399612725
190	.592186361	189.549558	.450442195
200	.624523739	199.519132	.480867982
210	.658437987	209.974853	.025146842
220	.692017099	220.327252	-.327252269
230	.724941184	230.477708	-.477707505
240	.757579774	240.540145	-.54014492
250	.789993373	250.533218	-.533217907
260	.82171493	260.312935	-.312934995
270	.853130175	269.998217	1.78325176E-03
280	.885509839	279.980828	.01917243

COEFF OF DETERM.=.99998048

COEFF OF CORREL.=.99999024

STD ERROR OF ESTIMATE=1.11869751E-03

Y(CALC)=-.0226378673+(3.24360677E-03*X)

X(CALC)=6.97922681+308.298777C1/C2

eqn #1
21 Dec 85

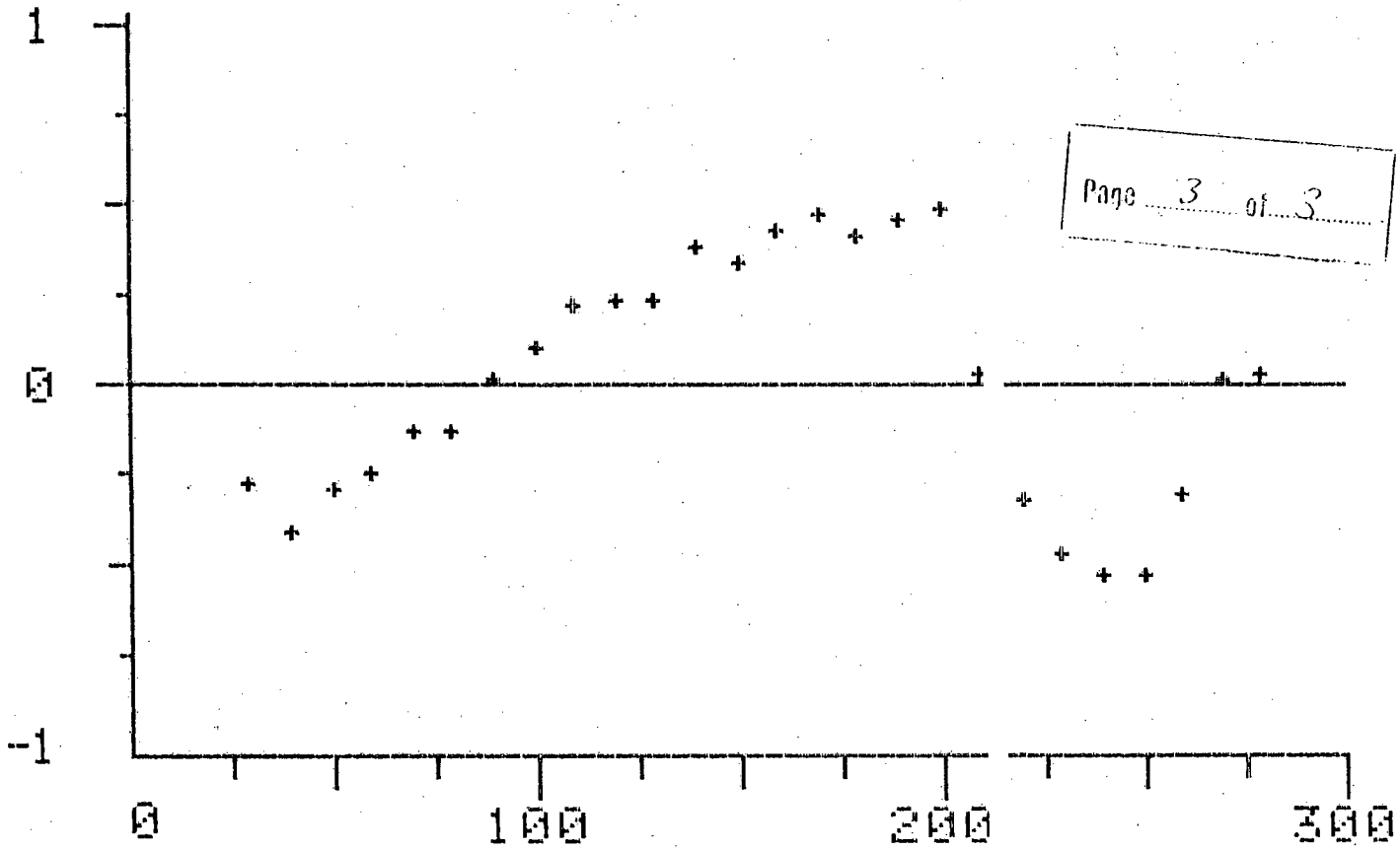

Page 3 of 3

CALIBRATION ERROR PLOT

SCALE IN cm DATE 21 DEC 85 TEMP NOT Rec.

REMARKS: Replaced 10 MHz crystal with 42 MHz crystal OUTPUT CHECKED AT 2 MHz, but varying in last 2 places.

#	X	C1	C2	C1/C2
1	60	1830	9982	.183329994
2	80	2479	9982	.248347025
3	100	3109	9979	.311554264
4	120	3765	9980	.377254509
5	140	4423	9984	.443008814
6	160	5087	9981	.50966837
7	180	5729	9978	.574163159
8	200	6352	9984	.636217949
9	220	7004	9978	.701944277
10	240	7656	9979	.767211143
11	260	8314	9978	.833233113

X(MEAS)	C1/C2	X(CALC)	XERR
60	.183329994	60.092621	-.0926210135
80	.248347025	80.1112351	-.111235052
100	.311554264	99.5726177	.42738238
120	.377254509	119.801592	.198408067
140	.443008814	140.047211	-.0472112298
160	.50966837	160.571555	-.571555316
180	.574163159	180.429372	-.429372013
200	.636217949	199.535918	.464082003
220	.701944277	219.772923	.227076948
240	.767211143	239.868461	.131539106
260	.833233113	260.196494	-.196493506

COEFF OF DETERM.=.999975483

COEFF OF CORREL.=.999987741

STD ERROR OF ESTIMATE=1.12444381E-03

Y(CALC)=-.0118405507+(3.24782879E-03*X)

X(CALC)=3.64568192+307.898003C1/C2

RUN # 1
16 Dec 85

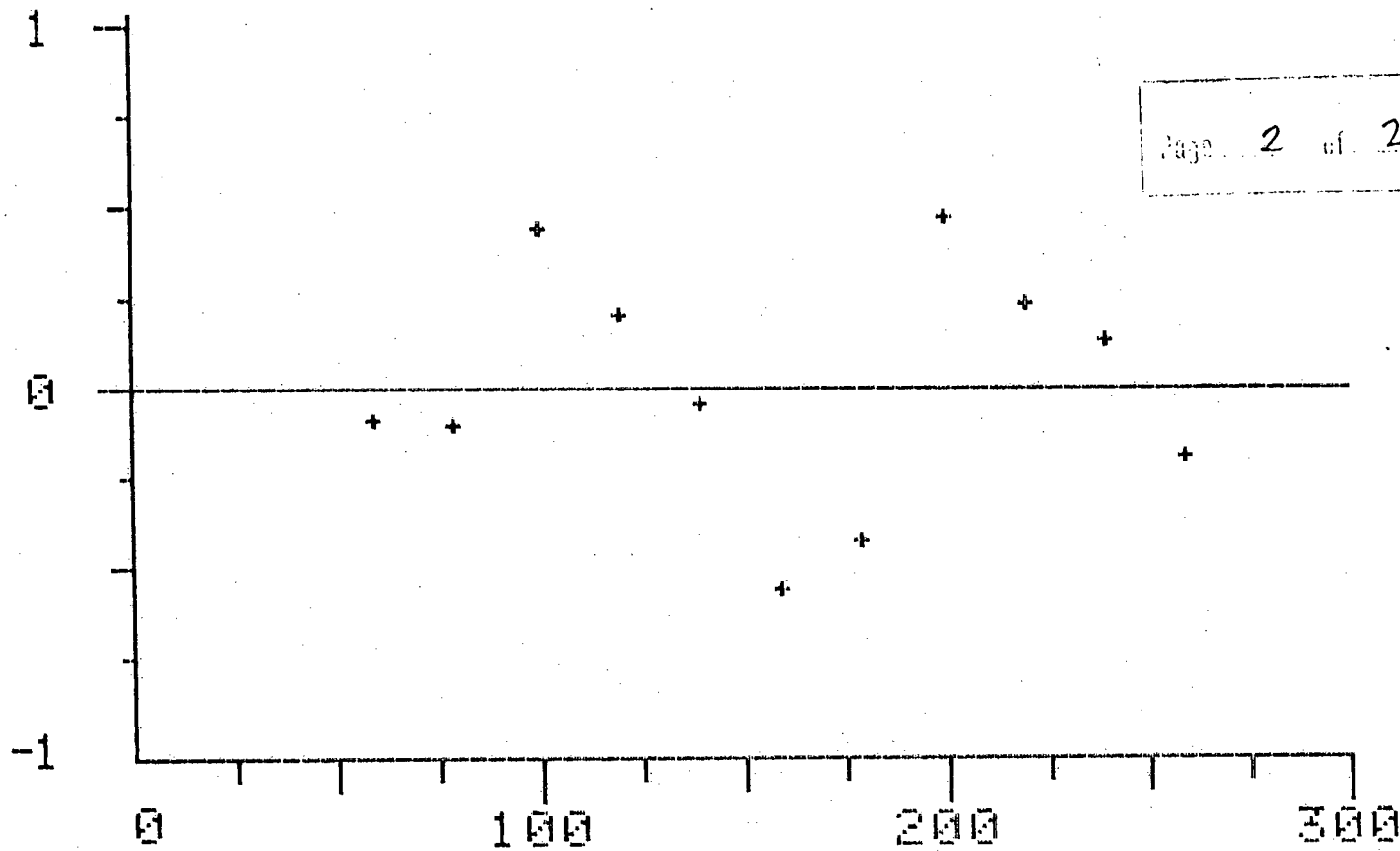

CALIBRATION ERROR PLOT

SCALE IN cm DATE 16 Dec 85 TEMP 24.5

REMARKS: Transmit pulse causing a ringing received pulse. 1st positive cycle smaller than second. Threshhold set low.

#	X	C1	C2	C1/C2
1	55	2004	10427	.192193344
2	75	2651	10428	.254219409
3	100	3457	10426	.331574909
4	125	4273	10428	.409762179
5	155	5245	10428	.502972766
6	170	5733	10429	.549717135
7	200	6700	10428	.642500959
8	225	7516	10427	.720820946
9	250	8322	10424	.798349962

X(MEAS)	C1/C2	X(CALC)	XERR
55	.192193344	55.0588798	-.0588798374
75	.254219409	75.0072841	-7.28404522E-03
100	.331574909	99.8858377	.114162385
125	.409762179	125.0319	-.0318995416
155	.502972766	155.009659	-9.65905189E-03
170	.549717135	170.043268	-.0432674289
200	.642500959	199.883774	.1162256
225	.720820946	225.07252	-.0725197792
250	.798349962	250.006878	-6.8783164E-03

COEFF OF DETERM.=.999998946

COEFF OF CORREL.=.999999473

STD ERROR OF ESTIMATE=2.29896838E-04

Y(CALC)=.0209974116+(3.10932465E-03*X)

X(CALC)=-6.75304574+321.613248C1/C2

RHN #2
16 Dec 85

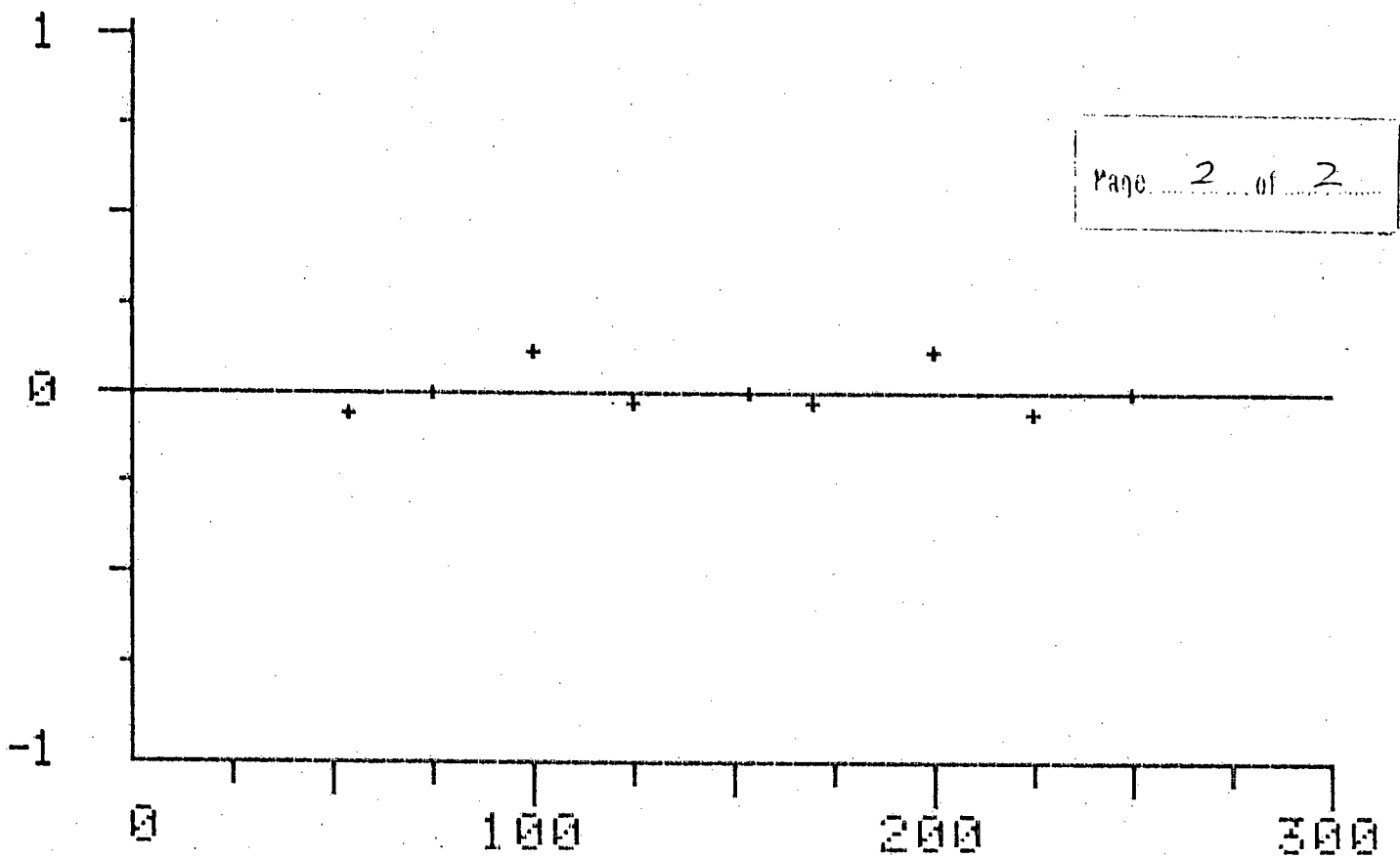

CALIBRATION ERROR PLOT

SCALE IN cm DATE 16DEC 85 TEMP 24

REMARKS: TRANSMIT PULSE ADJUSTED TO MAKE 1ST POSITIVE SWING LARGEST. COMPARATOR THRESHHOLD SET HIGH

27.946	Degrees	Hrs=	.01
26.918	Degrees	Hrs=	.00
26.887	Degrees	Hrs=	13.35
26.887	Degrees	Hrs=	13.81
26.757	Degrees	Hrs=	14.20
26.780	Degrees	Hrs=	14.66
26.785	Degrees	Hrs=	15.13
26.660	Degrees	Hrs=	15.59
26.398	Degrees	Hrs=	16.05
26.071	Degrees	Hrs=	16.35
25.884	Degrees	Hrs=	16.40
25.870	Degrees	Hrs=	16.86
25.756	Degrees	Hrs=	17.32
25.674	Degrees	Hrs=	17.79
25.598	Degrees	Hrs=	18.25
25.519	Degrees	Hrs=	18.71
25.356	Degrees	Hrs=	19.18
25.203	Degrees	Hrs=	19.64
25.045	Degrees	Hrs=	20.10
24.868	Degrees	Hrs=	20.57
24.833	Degrees	Hrs=	21.03
24.823	Degrees	Hrs=	21.49
24.778	Degrees	Hrs=	21.96
24.668	Degrees	Hrs=	22.42
24.645	Degrees	Hrs=	22.88
24.615	Degrees	Hrs=	23.35
24.466	Degrees	Hrs=	23.81
24.407	Degrees	Hrs=	24.27
24.326	Degrees	Hrs=	24.74
24.316	Degrees	Hrs=	25.20
24.332	Degrees	Hrs=	25.66
24.295	Degrees	Hrs=	26.13
24.283	Degrees	Hrs=	26.59
24.249	Degrees	Hrs=	27.05
24.243	Degrees	Hrs=	27.52
24.272	Degrees	Hrs=	27.98
24.244	Degrees	Hrs=	28.44
24.134	Degrees	Hrs=	28.91
23.899	Degrees	Hrs=	29.37
23.741	Degrees	Hrs=	29.83
23.636	Degrees	Hrs=	30.29
23.517	Degrees	Hrs=	30.76
23.614	Degrees	Hrs=	31.22
24.314	Degrees	Hrs=	31.68
25.327	Degrees	Hrs=	32.15
26.056	Degrees	Hrs=	32.61
26.440	Degrees	Hrs=	33.07
26.550	Degrees	Hrs=	33.54
26.684	Degrees	Hrs=	34.00
26.762	Degrees	Hrs=	34.46
26.763	Degrees	Hrs=	34.93
26.751	Degrees	Hrs=	35.39
26.807	Degrees	Hrs=	35.85
26.865	Degrees	Hrs=	36.32
26.889	Degrees	Hrs=	36.78
26.877	Degrees	Hrs=	37.24
26.865	Degrees	Hrs=	13.71
26.784	Degrees	Hrs=	14.17
26.704	Degrees	Hrs=	14.63
26.648	Degrees	Hrs=	15.10
26.609	Degrees	Hrs=	15.56
26.540	Degrees	Hrs=	16.02
26.399	Degrees	Hrs=	16.49
26.259	Degrees	Hrs=	16.95
26.036	Degrees	Hrs=	17.41

STABILITY RUN
17DEC85

```
22HR0
X = 199.779135 C1=6025    C2=9655    C1/C2=.624029
22HR30
X = 199.810041 C1=6026    C2=9655    C1/C2=.624132574
23HR0
X = 199.798423 C1=6025    C2=9654    C1/C2=.62409364
23HR30
X = 199.779135 C1=6025    C2=9655    C1/C2=.624029
0HR0
X = 199.810041 C1=6026    C2=9655    C1/C2=.624132574
0HR30
X = 199.790753 C1=6026    C2=9656    C1/C2=.624067937
1HR0
X = 199.810041 C1=6026    C2=9655    C1/C2=.624132574
1HR30
X = 199.821656 C1=6027    C2=9656    C1/C2=.6241715
2HR0
X = 199.810041 C1=6026    C2=9655    C1/C2=.624132574
2HR30
X = 199.810041 C1=6026    C2=9655    C1/C2=.624132574
3HR0
X = 199.821656 C1=6027    C2=9656    C1/C2=.6241715
3HR30
X = 199.810041 C1=6026    C2=9655    C1/C2=.624132574
4HR0
X = 199.798423 C1=6025    C2=9654    C1/C2=.62409364
4HR30
X = 199.821656 C1=6027    C2=9656    C1/C2=.6241715
5HR0
X = 199.829332 C1=6026    C2=9654    C1/C2=.624197224
5HR30
X = 199.821656 C1=6027    C2=9656    C1/C2=.6241715
6HR0
X = 199.840946 C1=6027    C2=9655    C1/C2=.624236147
6HR30
X = 199.852558 C1=6028    C2=9656    C1/C2=.624275062
7HR0
X = 199.77147  C1=6026    C2=9657    C1/C2=.624003314
7HR30
X = 199.759851 C1=6025    C2=9656    C1/C2=.623964374
8HR0
X = 199.736606 C1=6023    C2=9654    C1/C2=.623886472
8HR30
X = 199.74823  C1=6024    C2=9655    C1/C2=.623925427
9HR0
X = 199.71335  C1=6021    C2=9652    C1/C2=.623808537
9HR30
X = 199.759851 C1=6025    C2=9656    C1/C2=.623964374
10HR0
X = 199.744266 C1=6022    C2=9652    C1/C2=.623912143
10HR30
X = 199.736606 C1=6023    C2=9654    C1/C2=.623886472
```

Someone shut window after run started.

11HR0
X = 199.767514 C1=6024 C2=9654 C1/C2=.623990056
11HR30
X = 199.71335 C1=6021 C2=9652 C1/C2=.623808537
12HR0
X = 199.736606 C1=6023 C2=9654 C1/C2=.623886472
12HR30
X = 199.732638 C1=6021 C2=9651 C1/C2=.623873174
13HR0
X = 199.767514 C1=6024 C2=9654 C1/C2=.623990056
13HR30
X = 199.755891 C1=6023 C2=9653 C1/C2=.623951103
14HR0
X = 199.755891 C1=6023 C2=9653 C1/C2=.623951103
14HR30
X = 199.755891 C1=6023 C2=9653 C1/C2=.623951103
15HR0
X = 199.755891 C1=6023 C2=9653 C1/C2=.623951103
15HR30
X = 199.779135 C1=6025 C2=9655 C1/C2=.624029
16HR0
X = 199.767514 C1=6024 C2=9654 C1/C2=.623990056
16HR30
X = 199.779135 C1=6025 C2=9655 C1/C2=.624029
17HR0
X = 199.810041 C1=6026 C2=9655 C1/C2=.624132574
17HR30
X = 199.821656 C1=6027 C2=9656 C1/C2=.6241715

Page 1 of 2

STABILITY RUN
21 Dec 85
10 MHz XTAL
TROLLEY LOCKED AT 120cm.

START TIME = 19HR10

19HR40			
X = 119.910935	C1=2547	C2=6954	C1/C2=.366264021
20HR9			
X = 119.910935	C1=2547	C2=6954	C1/C2=.366264021
20HR39			
X = 119.955541	C1=2548	C2=6954	C1/C2=.366407823
21HR8			
X = 119.910935	C1=2547	C2=6954	C1/C2=.366264021
21HR38			
X = 119.910935	C1=2547	C2=6954	C1/C2=.366264021
22HR7			
X = 119.939199	C1=2548	C2=6955	C1/C2=.36635514
22HR37			
X = 119.939199	C1=2548	C2=6955	C1/C2=.36635514
23HR7			
X = 119.983799	C1=2549	C2=6955	C1/C2=.366498922
23HR37			
X = 119.983799	C1=2549	C2=6955	C1/C2=.366498922
0HR7			
X = 119.955541	C1=2548	C2=6954	C1/C2=.366407823
0HR37			
X = 119.955541	C1=2548	C2=6954	C1/C2=.366407823
1HR7			
X = 119.983799	C1=2549	C2=6955	C1/C2=.366498922
1HR37			
X = 119.983799	C1=2549	C2=6955	C1/C2=.366498922
2HR7			
X = 119.983799	C1=2549	C2=6955	C1/C2=.366498922
2HR37			
X = 119.967456	C1=2549	C2=6956	C1/C2=.366446233
3HR7			
X = 119.955541	C1=2548	C2=6954	C1/C2=.366407823
3HR37			
X = 119.983799	C1=2549	C2=6955	C1/C2=.366498922
4HR7			
X = 119.983799	C1=2549	C2=6955	C1/C2=.366498922
4HR37			
X = 119.983799	C1=2549	C2=6955	C1/C2=.366498922
5HR7			
X = 119.983799	C1=2549	C2=6955	C1/C2=.366498922
5HR37			
X = 119.983799	C1=2549	C2=6955	C1/C2=.366498922
6HR7			
X = 119.983799	C1=2549	C2=6955	C1/C2=.366498922
6HR37			
X = 119.983799	C1=2549	C2=6955	C1/C2=.366498922
7HR7			
X = 119.910935	C1=2547	C2=6954	C1/C2=.366264021
7HR37			

X = 119.838049 C1=2545 C2=6953 C1/C2=.366029052
8HR7
X = 119.838049 C1=2545 C2=6953 C1/C2=.366029052
8HR37
X = 119.793436 C1=2544 C2=6953 C1/C2=.365885229
9HR7
X = 119.809762 C1=2544 C2=6952 C1/C2=.36593786
9HR37
X = 119.838049 C1=2545 C2=6953 C1/C2=.366029052
10HR7
X = 119.838049 C1=2545 C2=6953 C1/C2=.366029052
10HR37
X = 119.866328 C1=2546 C2=6954 C1/C2=.366120219
11HR7
X = 119.866328 C1=2546 C2=6954 C1/C2=.366120219

Actual end time 11HR11 22 Dec 85
Low TEMP = 14.5
Hi Temp = 24
> D.H = 9.5

APPENDIX 10.4

REFERENCES

1. Thesis Number 3, An Ultrasonic Probe for the Measurement of the Temperature in an Arc Furnace, J.C. Niven, University of Cape Town, Undated.

2. Time Interval Measurement Between Two Ultrasonic Echoes, C.P. Vermaat, Thesis for BSc (ENG), University of Cape Town, Undated.

3. Pulse - Echo Method of Determining the Elastic Constants of Rectangular Strips and Square Plates, J.F.W. Bell and J.Y.F Chen, NDT International, December 1981.

4. Nickel and Nickel Alloys, an Extract From Metals Handbook, Ninth Edition, Volume 3, pages 125 to 182, American Society for Metals, 1985.

5. Handbook of Electronic Design and Analysis Procedures Using Programmable Calculators, Part 3 - Electromagnetic Component Design, Bruce K. Murdock, Van Nostrand Reinhold Company, New York, 1979.

6. Radio Engineering Handbook, 5th Edition, K. Henney, McGraw-Hill Book Company, New York, 1959.

7. IEEE Standard 488 - 1978, Institute of Electrical and Electronic Engineers, Inc., New York, November 30, 1978.

8. Apple II IEEE-488 Interface User's Guide, IEC 625, Apple Product # A2L0037, Cupertino, California, 1981.

9. Owner's Manual, Model 7490 GPIB Interface, California Computer Systems, Sunnyvale, California, 1980.

10. 96LS488 General Purpose Interface Bus (GPIB) Circuit, Fairchild Camera and Instrument Corporation, Mountain View, California, 1981.

11. PET/CBM and the IEEE 488 Bus (GPIB), 2nd Edition, Eugene Fisher and C.W. Jensen, Osborne/McGraw-Hill, Berkeley, California, 1982.

12. Science and Engineering Programs, Apple II Edition, Chapter 2 - Regression, John Heilborn, Osborn/McGraw-Hill, Berkeley, California, 1981.

APPENDIX 5

PHOTOCOPIES OF SELECTED PHOTOGRAPHS

Photograph Giving Overview of the Device Constructed on an Optical Bench

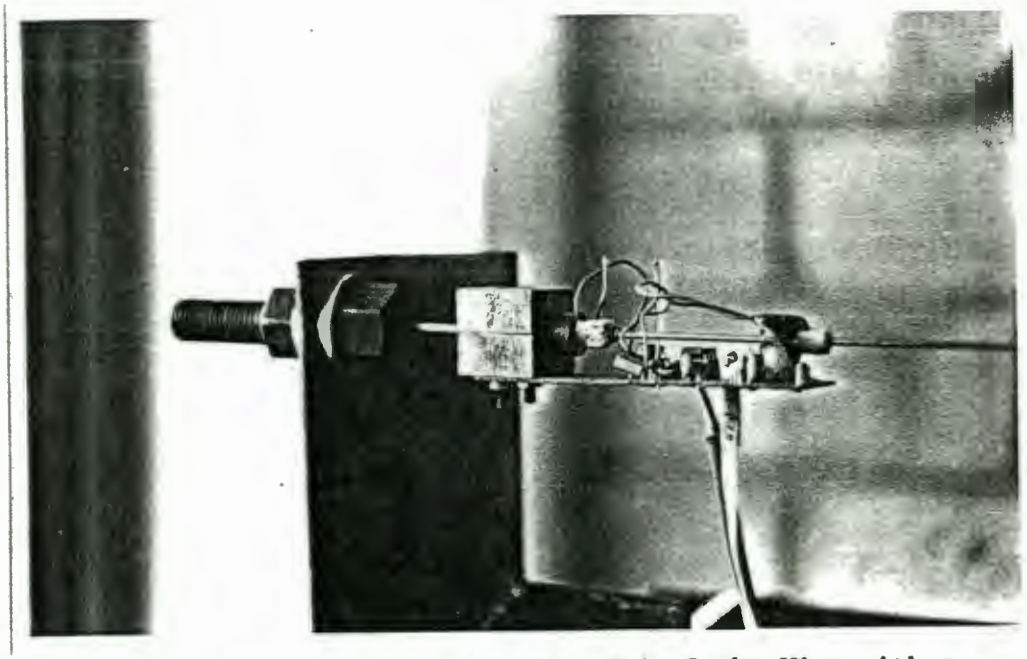

Photograph Showing One End of the Wire with a Reflecting Cube, Transmitting Coil, Fixed Receiving Coil and Preamplifier

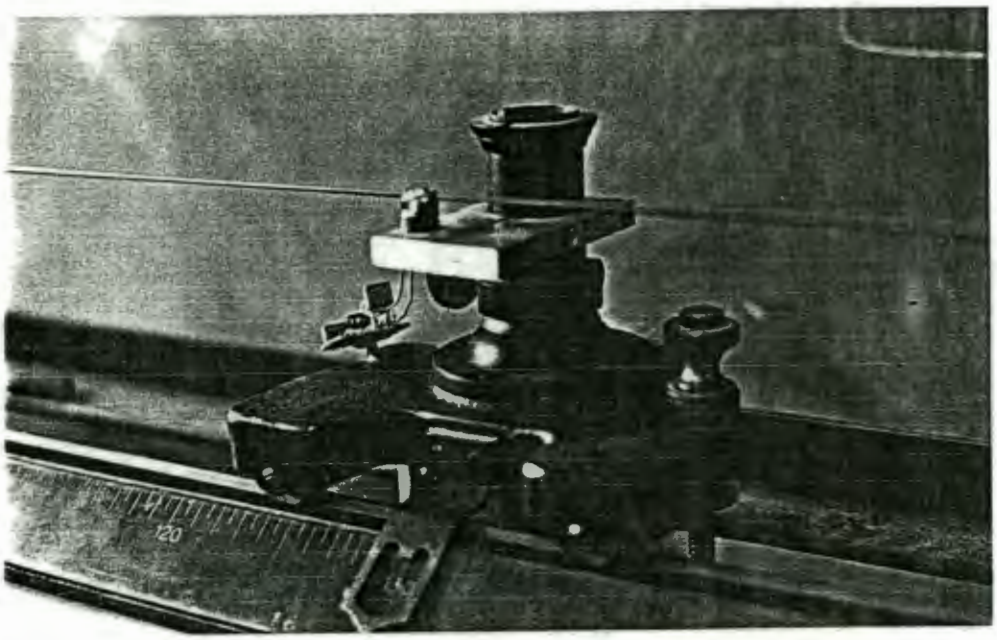

Photograph Showing the Moveable Coil Mounted on the Optical Bench Trolley

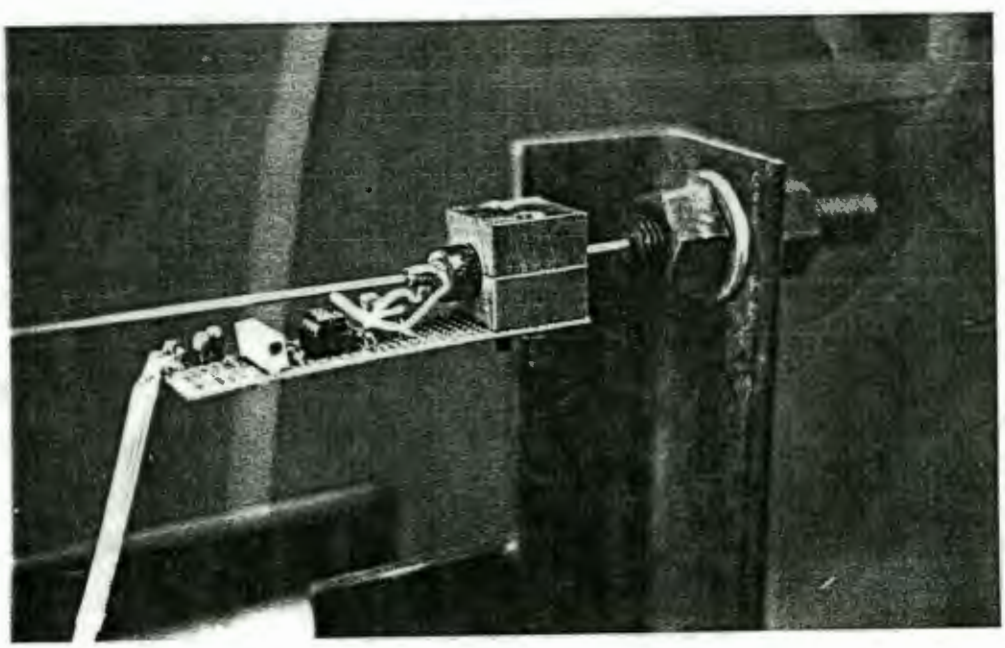

Photograph Showing the Other End of the Wire with a Reflecting Cube, Fixed Receiving Coil, Preamplifier and Tensioning Device

Photograph Showing the Electronics with Front Panel Signal Output and the Optical Bench in the Background

Photograph Showing a Typical Screen During Calibration